https://doi.org/10.5194/acp-2020-361
Preprint. Discussion started: 4 May 2020

Atmospheric Chemistry and Physics Discussions

Reappraising the appropriate calculation of a common meteorological quantity: Potential Temperature

Manuel Baumgartner[1,2], Ralf Weigel[2], Ulrich Achatz[4], Allan H. Harvey[3], and Peter Spichtinger[2]

[1]Zentrum für Datenverarbeitung, Johannes Gutenberg University Mainz, Germany
[2]Institute for Atmospheric Physics, Johannes Gutenberg University Mainz, Germany
[3]Applied Chemicals and Materials Division, National Institute of Standards and Technology, Boulder, CO, USA
[4]Institut für Atmosphäre und Umwelt, Goethe-Universität Frankfurt, Frankfurt am Main, Germany

Correspondence: Manuel Baumgartner (manuel.baumgartner@uni-mainz.de)

Abstract. The potential temperature is a widely used quantity in atmospheric science since it is conserved for air's adiabatic changes of state. Its definition involves the specific heat capacity of dry air, which is traditionally assumed as constant. However, the literature provides different values of this allegedly constant parameter, which are reviewed and discussed in this study. Furthermore, we derive the potential temperature for a temperature-dependent parameterization of the specific heat capacity of dry air, thus providing a new reference potential temperature with a more rigorous basis. This new reference shows different values and vertical gradients in the upper troposphere and the stratosphere compared to the potential temperature that assumes constant heat capacity. The application of the new reference potential temperature to the prediction of gravity wave breaking altitudes reveals that the predicted wave breaking height may depend on the definition of the potential temperature used.

1 Introduction

According to the book *Thermodynamics of the Atmosphere* by Alfred Wegener (1911), the first published use of the expression *potential temperature* in meteorology is credited to Wladimir Köppen (1888)[1] and Wilhelm von Bezold (1888), both following the conclusions of Hermann von Helmholtz (1888) (Kutzbach, 2016). Over 130 years ago, von Helmholtz perceived that within the atmosphere the heat exchange between air masses of different temperatures, which are relatively moved, is insufficiently explained by heat transfer due only to radiation and convection. He argued that wind phenomena (e.g., the trade winds), storm events, and the atmospheric circulation were more intense, of larger extent, and more persistent than observed if the air's heat exchange within the discontinuity region (the friction surface of the different air masses) was not mainly due to eddy-driven mixing. On his way to analytically describe the heat exchange of different air masses within the atmosphere, in May of 1880, von Helmholtz introduced the air's *immanent heat* while its absolute temperature changes with changing pressure (von Helmholtz, 1888). In essence, von Helmholtz concluded that the temperature gained by a volume of dry air due to its adiabatic descent from a certain initial pressure level (p) to ground pressure (p_0) corresponds to the air's immanent heat. In November of the same year, in agreement with von Helmholtz and probably inspired by a presentation that was given in

[1]In the publication year (1911) of Wegener's book, Köppen's daughter Else got engaged to Alfred Wegener (Reinke-Kunze, 2013) and they married in the year 1913 (Hallam, 1975).

https://doi.org/10.5194/acp-2020-361
Preprint. Discussion started: 4 May 2020


Atmospheric Chemistry and Physics Discussions

June by Köppen (1888), this property was renamed and reintroduced as the air's *potential temperature* (θ in the following) by von Bezold (1888) with the following definition for strictly adiabatic changes of state:

$$\theta = T\left(\frac{p_0}{p}\right)^{\frac{\gamma-1}{\gamma}}, \tag{1}$$

where T and p are the absolute temperature and pressure, respectively, of an air parcel at a certain initial (pressure-) altitude level. The quantities θ and p_0 are corresponding values of the same air parcel's absolute temperature and pressure if the air was exposed to conditions at ground level. The dimensionless coefficient γ, nowadays called the isentropic exponent, was specified as 1.41 (von Bezold, 1888).

Moreover, in the same publication, von Bezold concluded that for moist air's adiabatic changes of state, its potential temperature remains unchanged as long as the change of state occurs within dry-adiabatic limits; and further, if there is condensation and precipitation, the potential temperature changes by a magnitude that is determined by the amount of water that falls out of the air parcel. From a modern perspective, it is clear that the air parcel is an isolated thermodynamic system, and adiabatic processes correspond to processes with conserved entropy (i.e., isentropic processes). The description of the immanent heat is then equivalent to the thermodynamic state function entropy, which corresponds to potential temperature of dry air in a one-to-one relationship.

In general, the potential temperature has the benefit of providing a practicable vertical coordinate (equivalent to the pressure level or the altitude above, e.g., sea level) to visualise and analyse the vertical distribution and variability of (measured) data related to any type of atmospheric parameter. Admittedly, the use of the potential temperature as a vertical coordinate is initially less intuitive than applying altitude or pressure coordinates. Indeed, the potential temperature bears a certain abstractness to describe an air parcel's state at a certain altitude level by its imaginary dry-adiabatic descent to ground conditions. However, one major advantage of using the potential temperature as a vertical coordinate is that the (measured) data are sortable with respect to the entropy state at which the atmospheric samples were taken. Thus, the comparison of repeated measurements of an atmospheric parameter on an equipotential surface (isentrope) or layer excludes any diabatic change of the air parcel's state due to an entropy-changing uplift or descent of the air mass.

Apart from characterising the isentropes, the vertical profiles of the potential temperature (θ as a function of height z) are used as the reference for evaluating the atmosphere's actual vertical temperature gradient, which allows characterising its static stability. Notably, von Bezold (1888) already proposed the potential temperature as an atmospheric stability criterion. In its basic formulation, the potential temperature exclusively refers to the state of dry air, and thus the potential temperature characterises the atmosphere's static stability with respect to vertical displacements of a dry air parcel. In meteorology, the static stability parameter is expressed in terms of the (squared) Brunt-Väisälä frequency N in the form

$$N^2 = \frac{g}{\theta}\frac{\partial\theta}{\partial z}, \tag{2}$$

where g is the gravitational acceleration. The potential temperature twice enters the formulation of the stability parameter, as the denominator (θ^{-1}) and as the vertical gradient $\frac{\partial\theta}{\partial z}$. In the research field of dynamical meteorology, the potential vorticity (PV) is often used. The PV is proportional to the scalar product of the atmosphere's vorticity (the air's local spinning motion) and its

https://doi.org/10.5194/acp-2020-361
Preprint. Discussion started: 4 May 2020

Atmospheric Chemistry and Physics Discussions

stratification (the air's tendency to spread in layers of diminished exchange). More concretely, the PV is the scalar product of the absolute vorticity vector and the three-dimensional gradient of θ, i.e., not only the potential temperature's vertical gradient but also its partial derivatives on the horizontal plane add to the resulting PV, although, particularly at stratospheric altitudes, the vertical gradient constitutes the dominant contribution. For the analytical description of a fluid's motion within a rotational system, as is the atmosphere, the PV provides a quantity that varies exclusively due to diabatic processes. Occasionally, by means of the dynamical parameter PV, the tropopause height is defined (usually at 2 PV units, see, e.g., Gettelman et al., 2011) as is, e.g., the edge of a large-scale cyclone such as the polar winter vortex on specific θ levels (cf. Curtius et al., 2005).

While for a dry atmosphere (i.e., with little or no water vapour) the potential temperature is the correct conserved quantity (corresponding to entropy) for reversible processes, for an atmosphere containing water in two or more phases (vapour, liquid, and/or solid phases) energy transfers due to phase changes play a major role. Thus, the formulation of the potential temperature has to be extended (since entropy is still the right quantity for reversible processes, including phase changes). Starting from Gibbs' equation, some formulations are available, e.g., the entropy potential temperature defined by Hauf and Höller (1987) or more general versions as derived by Marquet (2011). In these formulations, phase changes and deviations from thermodynamic equilibrium are included. An approximation to these more general formulations is, e.g., the equivalent potential temperature, which includes latent heat release, assuming thermodynamic equilibrium (e.g., Emanuel, 1994). These formulations always rely on the assumption of reversible processes (i.e., conserved entropy). However, in the case of large hydrometeors, liquid or solid particles are removed due to gravitational acceleration, leading to an irreversible process. Sometimes for this situation a so-called pseudo adiabatic potential temperature is defined, assuming instantaneous removal of hydrometeors from the air parcel; usually, meaningful approximations to this quantity are given, since generally it cannot be derived from first principles. In a strict sense, this is not a conserved quantity, since an irreversible process is considered. Equivalent potential temperature including phase changes for vapour and liquid water is often used for the determination of convective instabilities. The general formulation can be easily adapted for an ice equivalent potential temperature, i.e., for reversible processes in pure ice clouds (see, e.g., Spichtinger, 2014). Although the latent heat of sublimation is larger than the latent heat of vaporisation, the absolute mass content of water vapour decreases exponentially with decreasing temperature, leading to only small corrections due to phase changes in pure ice clouds.

At altitudes above the clouds' top, within the upper troposphere and across the tropopause, the air is substantially dried out compared to tropospheric in-cloud conditions. Therefore, above clouds and further aloft, e.g., within the stratosphere, the conventional dry-air potential temperature may suffice to provide a meaningful vertical coordinate. Moreover, the potential temperature is commonly used as a prognostic variable in numerical models for the formulations of the energy equation. Thereby, very often both variants, the potential temperature as well as the equivalent potential temperature, are involved to account for dry air situations and cloud conditions.

In any case, the use of the potential temperature requires the following preconditions to be fulfilled:

1. θ should be based on a rigorous derivation to ensure its validity as a function of atmospheric altitude in order not to corrupt its character as a vertical coordinate that allows for appropriately comparing (measured) atmospheric parameters, and

https://doi.org/10.5194/acp-2020-361
Preprint. Discussion started: 4 May 2020


Atmospheric Chemistry and Physics Discussions

2. θ should approximate to the greatest possible extent the true entropy state of a probed air mass and should preferably account for the implied dependencies on atmospheric variables, even under the assumption that air behaves as an ideal gas,

with the aim that the potential temperature behaves as a rational physical variable. Thus, still abiding by the ideal gas assumption, a re-assessment of the fundamental atmospheric quantity θ is suggested, which is based on the state-of-knowledge of air's thermodynamic properties, and this re-assessed θ is comprehensively examined concerning its ability to hold also for atmospheric conditions above the troposphere.

In principle, the concept of the potential temperature is transferable to all systems of thermally stratified fluids as is a planetary gas atmosphere or an ocean, to investigate heat fluxes (advection or diffusion) or the static stability of the fluid. In astrophysics, the potential temperature is used almost identically as in atmospheric sciences to describe dynamic processes and thermodynamic properties (e.g. static stability or vorticity) in the atmosphere of planets other than the Earth. Here, the same value $p_0 = 1000\,\mathrm{hPa}$, as applied to the Earth's atmosphere, is frequently used as a reference pressure for the atmosphere of other planets (Catling, 2015, Table 4), whereby the formulations of the specific heat capacity require adaptations to account for the individual gas composition of the respective planetary atmosphere. The Weather Research and Forecasting model (WRF) was extended to "planetWRF" to simulate the weather in the atmosphere of other planets. Here, the potential temperature is included in the prognostic model equations (Richardson et al., 2007), while it was pointed out by Li and Chen (2019) that this approach could suffer from not accounting for the temperature dependence of the isobaric specific heat capacity c_p of the respective atmosphere's gas composition. The atmosphere of Jupiter's moon Titan, the only known moon with a substantial atmosphere, was comprehensively studied with frequent application of the potential temperature based on profile measurement of temperature and pressure in Titan's atmosphere by the Huygens-probe (Müller-Wodarg et al., 2014). Moreover, the potential temperature is a frequently used quantity in oceanography (e.g., McDougall et al., 2003; Feistel, 2008), while here the consideration of sea water's salinity and its impact on the specific heat capacity of sea water implies additional complexity. In particular, McDougall et al. (2003) suggests a re-assessment of the potential temperature as applied in oceanography to approximate the adiabatic lapse rate, thus this study bears certain parallels to the present investigation aiming at the reappraisal of the potential temperature for atmosphere-related purposes. These studies from other disciplines motivate the need for a re-assessment of the potential temperature for the atmospheric sciences. Thus, the approach provided herein proposes a modified calculation of the widely used quantity of the potential temperature by additionally accounting for the current state of knowledge concerning air's properties.

2 Derivation of the potential temperature for an ideal gas

The Gibbs equation (see, e.g., Kondepudi and Prigogine, 1998) is a general thermodynamic relation to describe the state of a system with m components and reads as

$$T\,\mathrm{d}S = \mathrm{d}H - V\,\mathrm{d}p - \sum_{k=1}^{m} \mu_k\,\mathrm{d}M_k, \tag{3}$$

https://doi.org/10.5194/acp-2020-361
Preprint. Discussion started: 4 May 2020


Atmospheric Chemistry and Physics Discussions

where T denotes the absolute temperature in K, S the entropy in $\mathrm{J\,K^{-1}}$, H the enthalpy in J, V the volume in $\mathrm{m^3}$, μ_k the chemical potential of component k in $\mathrm{J\,kg^{-1}}$, M_k the mass of component k in kg, and p the static pressure in Pa. Assuming no phase conversion or chemical reaction within the system, the mass of each component does not change, hence $\mathrm{d}M_k = 0$ for each component k.

In the following, dry air is assumed to be the single component in the system. Expressing the Gibbs equation in its specific form (i.e., division by the total mass M_a of dry air; note, lowercase letters indicate specific variables, e.g., $h = H/M_a$, etc.) leads to

$$T\,\mathrm{d}s = \mathrm{d}h - \frac{V}{M_a}\,\mathrm{d}p \quad \Leftrightarrow \quad \mathrm{d}s = \frac{1}{T}\,\mathrm{d}h - \frac{V}{M_a T}\,\mathrm{d}p. \tag{4}$$

Furthermore, approximating dry air as an ideal gas leads to the following simplifications:

- The ideal gas law

  $$pV = M_a R_a T \tag{5}$$

  can be applied with the specific gas constant R_a of dry air, which is

  $$\begin{aligned} R_a &= \frac{R}{M_{\mathrm{mol},a}} \\ &= \frac{8.31446261815324\,\mathrm{J\,mol^{-1}K^{-1}}}{0.0289586\,\mathrm{kg\,mol^{-1}} \pm 0.0000002\,\mathrm{kg\,mol^{-1}}}, \end{aligned} \tag{6}$$

  where R is the molar gas constant in $\mathrm{J\,mol^{-1}K^{-1}}$ (Tiesinga et al., 2020; Newell et al., 2018) and $M_{\mathrm{mol},a}$ is the molar mass of dry air (Lemmon et al., 2000), composed of nitrogen $\mathrm{N_2}$, oxygen $\mathrm{O_2}$, and argon Ar.

- The specific enthalpy is given by

  $$\mathrm{d}h = c_p\,\mathrm{d}T \tag{7}$$

  with c_p the specific heat capacity of dry air.

Based on these assumptions, the change of the specific entropy (within the fluid *dry air*) is given by

$$\mathrm{d}s = \frac{c_p}{T}\,\mathrm{d}T - R_a\frac{\mathrm{d}p}{p}. \tag{8}$$

For isentropic changes of state, i.e., $\mathrm{d}s = 0$, equation (8) reduces to

$$\frac{c_p}{T}\,\mathrm{d}T = R_a\frac{\mathrm{d}p}{p}. \tag{9}$$

Note that the assumption of dry air being an ideal gas does not imply that in (9) the specific heat capacity c_p is constant. While statistical mechanics excludes any pressure dependence in the ideal-gas heat capacity, the general derivation (cf. Appendix A) permits a temperature dependence of c_p. However, usually the temperature dependence is neglected in atmospheric physics

https://doi.org/10.5194/acp-2020-361
Preprint. Discussion started: 4 May 2020


Atmospheric Chemistry and Physics Discussions

and, instead, c_p is assumed as constant. Immediately below and in Section 3, the treatment of c_p as a temperature-independent constant is discussed. The introduction of the temperature dependence then follows in Section 4.

Treating c_p as a constant, rearrangement of (9) leads to

$$\frac{\mathrm{d}T}{T} = \frac{R_a}{c_p}\frac{\mathrm{d}p}{p}. \tag{10}$$

Integration of (10) over the range from ground-level pressure and temperature (p_0, T_0) to the pressure and temperature at a specific height (p, T) yields

$$\ln\left(\frac{T}{T_0}\right) = \int_{T_0}^{T}\frac{\mathrm{d}T'}{T'} = \frac{R_a}{c_p}\int_{p_0}^{p}\frac{\mathrm{d}p'}{p'} = \frac{R_a}{c_p}\ln\left(\frac{p}{p_0}\right), \tag{11}$$

and, after another straightforward conversion, one arrives at

$$\ln\left(\frac{T_0}{T}\right) = \frac{R_a}{c_p}\ln\left(\frac{p_0}{p}\right). \tag{12}$$

With the definition $\theta_{c_p} = T_0$, equation (12) is transformed into the commonly used expression for determining the potential temperature

$$\theta_{c_p} = T\left(\frac{p_0}{p}\right)^{\frac{R_a}{c_p}}, \tag{13}$$

for which the ground-level pressure p_0 is arbitrary but usually set to $p_0 = 1000\,\mathrm{hPa}$. This choice coincides with the definition of the World Meteorological Organisation (WMO, 1966) and the standard-state pressure (Tiesinga et al., 2020), but should not be confused with the standard atmosphere $101325\,\mathrm{Pa}$ (Tiesinga et al., 2020). In the following, θ_{c_p} denotes the potential temperature based on a constant c_p and, when a specific value of c_p is applied, the subscript c_p in the potential temperature's notation is replaced by the corresponding c_p value.

3 Examining the assumption of constant c_p for dry air

The general theory of thermodynamics, assuming dry air as an ideal gas, gives the expression

$$c_p = \left(1 + \frac{f}{2}\right) R_a \tag{14}$$

for the constant specific heat capacity, which is based on the results of statistical mechanics and the equipartition theorem (e.g., Huang, 1987). In (14), the parameter $f = f_{\mathrm{trans}} + f_{\mathrm{rot}} + f_{\mathrm{vib}}$ is equal to the total number of degrees of freedom of the gas molecules of which dry air consists. The individual contributions to f comprise the degrees of freedom of translation f_{trans}, rotation f_{rot}, and vibration f_{vib}. Assuming further that dry air exclusively consists of the linear molecules $\mathrm{N_2}$ and $\mathrm{O_2}$ (implying $f_{\mathrm{trans}} = 3$ and $f_{\mathrm{rot}} = 2$, while the contribution of Ar remains disregarded) and additionally neglecting the vibrational degrees of freedom ($f_{\mathrm{vib}} = 0$), the general relation (14) reduces to

$$c_p = \left(1 + \frac{3+2}{2}\right) R_a = \frac{7}{2} R_a. \tag{15}$$

https://doi.org/10.5194/acp-2020-361
Preprint. Discussion started: 4 May 2020

Atmospheric Chemistry and Physics Discussions

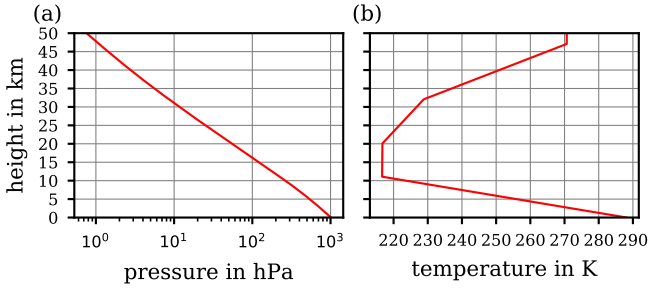

Figure 1. Vertical profiles of (a) atmospheric pressure and (b) temperature as functions of height, corresponding to the US Standard Atmosphere.

Although the neglect of vibrational excitation, particularly at very low temperatures, seems plausible and appropriate, errors are already introduced by this assumption for the temperature range relevant in the atmosphere.

In atmospheric sciences, for the majority of computations that require the specific heat capacity of dry air, a constant value of c_p may be appropriate. According to the WMO (1966), the recommended value for c_p of dry air is $1005\,\mathrm{J\,kg^{-1}K^{-1}}$ and, furthermore (*ibid.*), it is defined that $\gamma = \frac{c_p}{c_v} = \frac{7}{5} = 1.4$, cf. (1). This definition is consistent with the general thermodynamic theory together with all aforementioned additional assumptions and results in (15) as well.

Even assuming a universally valid constant c_p, a single consistently used value of c_p was not found. Instead, the specified values of c_p vary among different textbooks and other sources. In Table 1, some of the available values of constant specific heat capacity for dry air are compiled, indicating a variability of c_p that ranges from $994\,\mathrm{J\,kg^{-1}K^{-1}}$ to $1011\,\mathrm{J\,kg^{-1}K^{-1}}$.

These different values of constant c_p scatter within a small range (below $\pm 1.1\,\%$) around the WMO's recommendation $1005\,\mathrm{J\,kg^{-1}K^{-1}}$, which may seem negligible if c_p contributes only as a linear coefficient within an equation (e.g., in the expression of the correction factor ξ, cf. Weigel et al., 2016). Unfortunately, however, in the formulation of the potential temperature θ_{c_p}, cf. (13), the specific heat capacity c_p does not contribute linearly but rather as the denominator in the exponent. Thus, the variety of different c_p values, although scattering within a small range, impacts the resulting θ_{c_p} significantly. To quantify this impact, a computation of θ_{c_p} by using (13) was based on the values of static pressure (p, cf. Figure 1a) and absolute temperature (T, cf. Figure 1b) corresponding to the US Standard Atmosphere (United States Committee on Extension to the Standard Atmosphere, 1976).

From the list of the different c_p (cf. Table 1), two extreme values were selected, namely $994\,\mathrm{J\,kg^{-1}K^{-1}}$ (Wegener and Wegener, 1935) and $1011\,\mathrm{J\,kg^{-1}K^{-1}}$ (WMO, 1966), in order to initially illustrate the sensitivity of the resulting θ_{c_p} to variations in c_p in the range of $\sim 1\%$, as referenced by literature. Specific distinctions will be discussed at a later stage, then mainly in relationship to the commonly used recommendation of the WMO ($c_p = 1005\,\mathrm{J\,kg^{-1}\,K^{-1}}$, WMO, 1966). In Figure 2a, the individual profiles of θ_{c_p} are shown, and panel (b) exhibits the absolute difference $\Delta\theta_{c_p} = \theta_{994} - \theta_{1011}$, based on the c_p values selected. Figure 2b shows the sensitive response of calculated θ_{c_p} to a small variability in c_p. At an altitude of $5\,\mathrm{km}$, the difference $\Delta\theta_{c_p}$ already exceeds $1\,\mathrm{K}$. The values of $\Delta\theta_{c_p}$ reach approximately $2.5\,\mathrm{K}$ at $10\,\mathrm{km}$ altitude and rise further, above

https://doi.org/10.5194/acp-2020-361
Preprint. Discussion started: 4 May 2020

Atmospheric Chemistry and Physics Discussions

constant dry air's specific heat capacity c_p in $\mathrm{J\,kg^{-1}K^{-1}}$	literature source
994	Wegener and Wegener (1935) (converted from units other than SI)
1000	Vallis (2006) Roedel and Wagner (2011)
1003	"minimum of range of actual values" (WMO, 1966) Tripoli and Cotton (1981)
1004	Holton (2004) Wallace and Hobbs (2006) Schumann (2012) Wendisch and Brenguier (2013)
1004.8	Pruppacher and Klett (2010) (converted from units other than SI)
1005	recommended by WMO (1966) Bohren et al. (1998) Houghton (2002) Zdunkowski and Bott (2003) Brasseur and Solomon (2005) Seinfeld and Pandis (2006) Cotton et al. (2010)
1005.7 ± 2.5	Bolton (1980) Emanuel (1994)
1006	Wendisch and Brenguier (2013) (potential typo on p.69, a smaller value, cf. above, is given on p.24 and in the list of constants)
1011	"maximum of range of actual values" (WMO, 1966)

Table 1. Temperature-independent constant values given mainly in textbooks for the specific heat capacity c_p of dry air.

https://doi.org/10.5194/acp-2020-361
Preprint. Discussion started: 4 May 2020

Atmospheric Chemistry and Physics Discussions

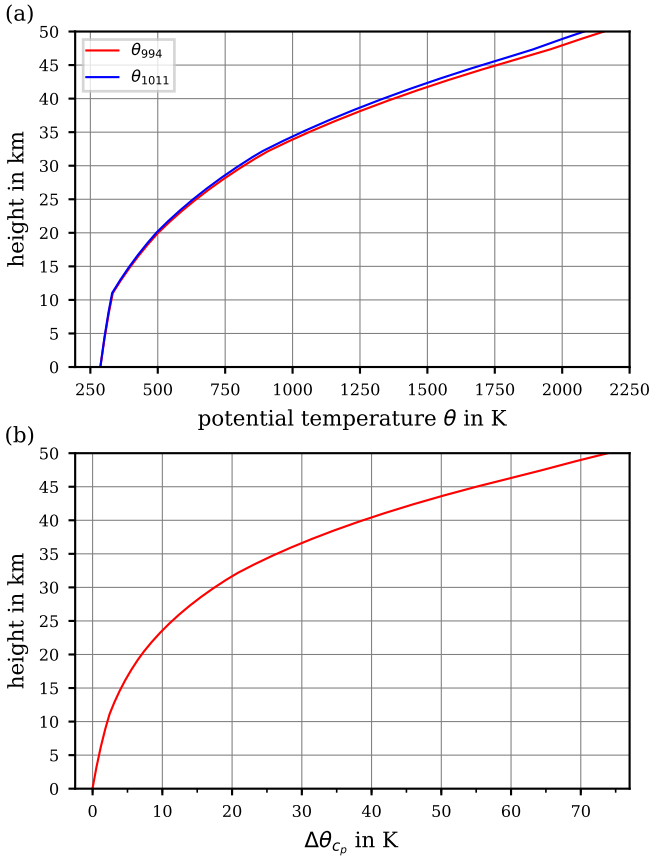

Figure 2. Computed vertical course of the potential temperature θ_{c_p} based on the two extremes of constant values for the specific heat capacity c_p provided in the literature (panel (a); cf. also Table 1), and (b) the absolute difference $\Delta\theta_{c_p} = \theta_{994} - \theta_{1011}$ between the two resulting curves of θ_{c_p}.

7 K, with increasing altitude up to 20 km. At 50 km, approximately where the stratopause is located, which is the chosen upper height limit for this investigation, the computed $\Delta\theta_{c_p}$ reaches almost 75 K.

The impact of this sensitivity becomes important at altitudes of ~ 10 km and above, thus, where the use of the potential temperature becomes increasingly meaningful. Here, and in particular above the cloud tops, the small-scale and comparatively fast tropospheric dynamics (causing vertical transport and implying diabatic processes) become diminished, while further above, towards the stratosphere, an increasingly layered vertical structure of the atmosphere is taking over.

As discussed above, the potential temperature is remarkably sensitive to small variations (within the per-cent range) of air's specific heat capacity, as these variations affect the exponent of the equation for θ_{c_p}; further proof of this, from the mathematical perspective, is provided in Appendix B. The studies of Ooyama (1990, 2001) document an interesting attempt to formulate, e.g., the energy balance equations for the moist atmosphere, wherein entropy replaces the more common formulation using the potential temperature. This substitution avoids the use of the potential temperature, which "is merely an exponential transform

https://doi.org/10.5194/acp-2020-361
Preprint. Discussion started: 4 May 2020


Atmospheric Chemistry and Physics Discussions

of the entropy expressed in units of temperature" (Ooyama, 2001), thus, within this equation, air's specific heat capacity is implied exclusively as a linear coefficient. Consequently, a parameterisation for the temperature dependence of the specific heat capacity ($c_p(T)$, cf. Section 4) may be easily adopted. However, the crucial drawback of the entropy-based equations is that to gain a numerical model for, e.g., weather forecast purposes, the parameterisations of most of the physical processes within the atmosphere would require a reformulation.

It should be noted that not only do literature values of air's specific heat capacity c_p vary, but also the values of the gas constant R_a vary slightly due to different historical approximations for the molar gas constant R and for the composition of dry air. The variation of values for R_a is typically only on the order of $10^{-1}\,\mathrm{J\,kg^{-1}K^{-1}}$, whereas the variability in c_p is on the order of a few $\mathrm{J\,kg^{-1}K^{-1}}$ (cf. Table 1). Therefore, within the exponent of the expression (13) for θ_{c_p}, the variability of c_p has by far a stronger impact on the resulting θ_{c_p} value than the variability of R_a.

However, accepting for a moment the WMO's definition (15) of c_p (WMO, 1966), the variability of air's c_p should naturally be constrained to certain limits. With the specific gas constant $R_a = 287.05\,\mathrm{J\,kg^{-1}K^{-1}}$ (WMO, 1966), the WMO's definition leads to $c_p = 1004.675\,\mathrm{J\,kg^{-1}K^{-1}}$. In contrast, taking into account the uncertainty introduced in R_a by the molar mass of dry air, cf. Equation (6), the resulting range for air's specific heat capacity is $1004.897\,\mathrm{J\,kg^{-1}K^{-1}} \leq c_p \leq 1004.912\,\mathrm{J\,kg^{-1}K^{-1}}$. It may be surmised that the rounded value $c_p = 1005\,\mathrm{J\,kg^{-1}K^{-1}}$ as recommended by the WMO (1966) had the main goal to simplify certain calculations, which at the time may have been mostly done by hand.

4 Accounting for the temperature dependence of air's specific heat capacity

Next, while retaining the ideal-gas assumption, we consider the dependence of air's c_p on temperature over the atmospherically relevant range ($180\,\mathrm{K}$ to $300\,\mathrm{K}$). The temperature dependence of c_p is, of course, not a new finding. Experimental approaches for determining the calorimetric properties of air and the temperature dependence of a fluid's specific heat capacity are described by Witkowski (1896), who investigated the change of the mean c_p as a function of temperature intervals between room temperature (as a fixed reference) and various warmer and colder temperatures, for atmospheric pressures and slightly beyond. Despite the potentially high uncertainty of the experimental results from these times, Witkowski (1896) already indicated that with decreasing temperature the experimentally determined c_p values initially decline, then pass a minimum, and subsequently increase again at lower temperatures ($T < 170\,\mathrm{K}$). The description of refined experiments and ascertainable data of air's $c_p(T)$ for temperatures below $293\,\mathrm{K}$ is summarised by Scheel and Heuse (1912), Jakob (1923), and Roebuck (1925, 1930), illustrating in comprehensive detail the experimental effort and providing the resulting data. The review by Awano (1936) compiled and compared the data of $c_p(T)$ of dry air ("*air containing neither carbon-dioxide nor steam*", Awano, 1936) and he attested—at that time—the previously mentioned studies to constitute "*the most reliable experiments*". During the decades following these experiments, further insights were gained and landmarks were reached which are summarised in the comprehensive survey by Lemmon et al. (2000) of the progress of modern formulations for the thermodynamic properties of air and about the experiments the previous formulations were based on.

https://doi.org/10.5194/acp-2020-361
Preprint. Discussion started: 4 May 2020

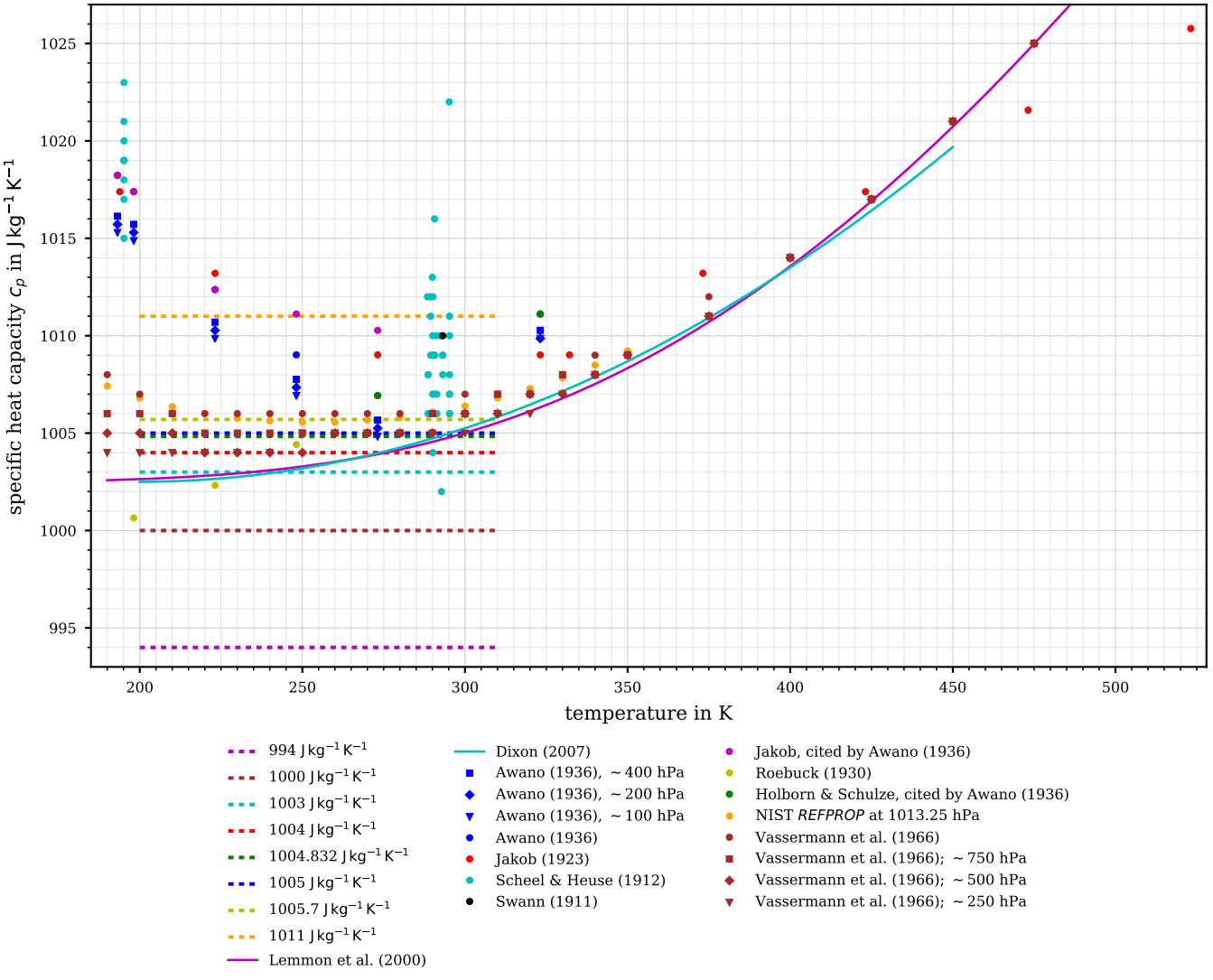

Figure 3. Variety of suggested values for the specific heat capacity of air. Constant values of c_p are displayed over the range documented in Table 1 (dashed lines). The parameterisations of air's $c_p(T)$, accounting for its temperature dependence by Lemmon et al. (2000, solid magenta curve) and by Dixon (2007, solid cyan curve) are displayed. Discrete measurement and literature data at about 1000 hPa (i.e., as often specified, at *about one atmosphere*) are indicated by dots. In addition, the studies by Awano (1936) and Vasserman et al. (1966) provide data at other atmospheric pressures, as indicated by squares, diamonds, and triangles.

https://doi.org/10.5194/acp-2020-361
Preprint. Discussion started: 4 May 2020


Atmospheric Chemistry and Physics Discussions

Figure 3 illustrates the range of suggested constant values for the specific heat capacity (see Table 1) together with the measurements that were made to obtain air's behaviour as a function of temperature and pressure. In the same figure, calculated values of $c_p(T)$ of dry air are displayed resulting from the equation of state which was derived from experimental p, V, and T data by Vasserman et al. (1966), who provided an extensive review of previous experimental and theoretical works and of the state of knowledge at that time. In addition, Figure 3 exhibits two different parameterisations, by Lemmon et al. (2000) and by Dixon (2007), which account for the temperature dependence of the specific heat capacity $c_p(T)$. Moreover, Figure 3 contains discrete values of dry air's $c_p(T)$ extracted from the database *REFPROP* (Reference Fluid Thermodynamic and Transport Properties Database by NIST, the National Institute of Standards and Technology, Lemmon et al., 2018), which is based on parameterisations resulting from thermodynamic considerations discussed later.

The measurement data, as well as the parameterisations, clearly indicate a dependence of air's specific heat capacity on the temperature. At temperatures above $300\,\mathrm{K}$, the data points by Jakob (1923) are surprisingly well captured by the parameterisations, while below $270\,\mathrm{K}$ the course of the parameterised and measured $c_p(T)$ diverge significantly. Possible reasons for this include:

- the measurements of $c_p(T)$ have a precision likely no better than $1\,\%$, and there could be systematic errors, especially at low temperatures;
- the measured data reflect the true thermodynamic behaviour of the real gas, rather than that of an ideal gas.

However, it is immediately obvious from Figure 3 that a good agreement among (i) the experimentally determined $c_p(T)$ data, (ii) a constant c_p (e.g., $1005\,\mathrm{J\,kg^{-1}K^{-1}}$; WMO (1966)), and (iii) the parameterised $c_p(T)$ is found only for a temperature interval ranging from $270\,\mathrm{K}$ to $290\,\mathrm{K}$. For all air temperatures below $270\,\mathrm{K}$, the constant value $c_p = 1005\,\mathrm{J\,kg^{-1}K^{-1}}$ fails to coincide with either the parameterised or the experimentally determined values of $c_p(T)$.

4.1 The temperature dependence of the ideal-gas specific heat capacity

As already indicated by the data depicted in Figure 3, the specific heat capacity c_p depends on the gas temperature. With regard to measured values, the lack of constancy may be due to real-gas effects or to a dependence of the ideal-gas heat capacity on temperature. In this section, we focus on the latter effect, denoting the ideal-gas isobaric specific heat capacity by $c_p^0(T)$, where the superscript 0 indicates the underlying ideal-gas assumption. For an individual gas, there is always a contribution from the three translational degrees of freedom, $c_{p,\mathrm{trans}}^0 = \frac{5}{2} R_i$, where R_i is the specific gas constant of the gas. If the molecule is assumed to be a rigid rotor, there is also a rotational contribution given by

$$c_{p,\mathrm{rot}}^0 = \begin{cases} R_i, & \text{for linear (e.g., diatomic) molecules,} \\ \frac{3}{2} R_i, & \text{for nonlinear molecules.} \end{cases} \tag{16}$$

As mentioned previously, at finite temperatures molecules also have contributions to $c_p^0(T)$ from intramolecular vibrations (and, at high temperatures, excited electronic states). To arrive at a temperature-dependent parameterisation for the ideal-gas specific heat capacity of dry air, the compounds' individual contributions, considering all degrees of freedom, need to

https://doi.org/10.5194/acp-2020-361
Preprint. Discussion started: 4 May 2020


Atmospheric Chemistry and Physics Discussions

be parameterised and then combined according to each compound's proportion in the mixture. For the following, dry air is considered a three-component mixture: the diatomic gases nitrogen (N_2) and oxygen (O_2) and the monatomic gas argon (Ar).

To determine the contribution of N_2 to $c_p^0(T)$, both Bücker et al. (2002) and Lemmon et al. (2000) use the ideal-gas heat capacity from the reference equation of state of Span et al. (2000) that compares well with the findings from other studies within an uncertainty Δc_p^0 of less than $0.02\,\%$.

For the contribution of O_2, Lemmon et al. (2000) use the formulation given by Schmidt and Wagner (1985). Alternatively, Bücker et al. (2002) provide a slightly different formulation from the International Union of Pure and Applied Chemistry (IUPAC, Wagner and de Reuck, 1987), after refitting it to more recently obtained data, thereby achieving an overall uncertainty Δc_p^0 of less than $\pm 0.015\,\%$ for O_2 (Bücker et al., 2002). However, the difference in the resulting specific heat capacity contribution by O_2 between the two approaches (Lemmon et al. (2000) or Bücker et al. (2002)) is comparatively small.

For a monoatomic gas such as Ar, vibrational and rotational contributions to the heat capacity do not exist, and Bücker et al. (2002) consider that argon's excited electronic states are relevant only at temperatures above $3500\,\mathrm{K}$. Hence, the contribution of argon Ar to the specific heat capacity of air reduces to $c_p^0 = \frac{5}{2} R_{\mathrm{Ar}}$.

The approach by Bücker et al. (2002) additionally considers the contribution of further constituents of air, such as water, carbon monoxide, carbon dioxide, and sulfur dioxide. These authors provide an analytical expression for specific heat capacity, accounting for this more complex but proportionally invariant air composition which is specified to deviate from the used reference by $\Delta c_p^0 \leq \pm 0.015\,\%$ in the temperature range of $200\,\mathrm{K} \leq T \leq 3300\,\mathrm{K}$. At atmospheric altitudes above the clouds' top, i.e., on average above $\sim 11\,\mathrm{km}$, the air is assumed to have lost most of its water and is deemed as dry. Furthermore, for the following, trace gases that contribute to air's composition by molar fractions of less than that of Ar are neglected.

4.2 NIST's parameterisation of $c_p^0(T)$

Besides a comprehensive survey of the available experimental data for the specific heat capacity of air, Lemmon et al. (2000) also provide state-of-the-art knowledge for other thermodynamic properties (isochoric heat capacity, speed of sound, vapour-liquid-equilibrium, etc.). Additionally, they give two approaches to derive air's thermodynamic properties, including the vapour-liquid equilibrium:

1. an empirical model-based *equation of state* for standard (dry) air considered as a pseudo-pure fluid, and
2. assembly of a *mixture model* from equations of state for each pure fluid.

Each approach allows calculating the thermodynamic properties, e.g., c_p, of gas mixtures such as dry air, and both are real-gas models with the ideal-gas behaviour as a boundary condition. The major difference between the models is that the first approach considers air as a pseudo-pure fluid while the second, more rigorous approach treats air as a mixture composed of N_2, O_2, and Ar, in molar fractions of 0.7812, 0.2096, and 0.0092, respectively, following Lemmon et al. (2000, their table 3). This fractional composition of dry air is assumed to be constant from ground level up to $80\,\mathrm{km}$ height (United States Committee on Extension to the Standard Atmosphere, 1976) and its fractional composition would have to be shifted significantly to cause a serious deviation of the resulting potential temperature. The contribution to the composition by carbon dioxide (CO_2) and of

https://doi.org/10.5194/acp-2020-361
Preprint. Discussion started: 4 May 2020

Atmospheric Chemistry and Physics Discussions

any other trace species was assumed to be negligible. The validity of both approaches is specified for various states of dry air, from its solidification point (59.75 K) up to temperatures of 1000 K, and for pressures up to 100 MPa and even much further beyond the pressure range that is relevant for atmospheric investigations. Both the pseudo-pure fluid model and the mixture model are implemented in NIST's *REFPROP* database (cf. https://www.nist.gov/srd/refprop) for various physical properties of fluids over a wide range of temperatures and pressures. Lemmon et al. (2000) suggest that their mixture models allow calculation of the specific heat capacity of a gas mixture within an estimated uncertainty of 1 %.

Both the pseudo-pure fluid model and the mixture model of Lemmon et al. (2000) use the same expression for the ideal-gas heat capacity, which is rigorously given as a sum of the pure-component contributions:

$$\begin{aligned}\frac{C_p^0(T)}{R} = {} & x_{\mathrm{N_2}} \left(\frac{C_p^0(T)}{R} \right)_{\mathrm{N_2}} + x_{\mathrm{Ar}} \left(\frac{C_p^0(T)}{R} \right)_{\mathrm{Ar}} \\ & + x_{\mathrm{O_2}} \left(\frac{C_p^0(T)}{R} \right)_{\mathrm{O_2}},\end{aligned} \tag{17}$$

where x_i denotes the molar fraction of species i, and C_p^0 as well as the molar gas constant R are given in units of $\mathrm{J\,mol^{-1}K^{-1}}$.

Like Bücker et al. (2002), Lemmon et al. (2000) use the expression of Span et al. (2000) for the contribution of $\mathrm{N_2}$ to the heat capacity and adopt $C_p^0 = \frac{5}{2}R$ for Ar. Together with the contribution by $\mathrm{O_2}$ according to the formulation by Schmidt and Wagner (1985), the expression provided by Lemmon et al. (2000) for the ideal-gas heat capacity of dry air is

$$\begin{aligned}\frac{C_p^0(T)}{R} = {} & N_1 + N_2 T + N_3 T^2 + N_4 T^3 + N_5 T^{-\frac{3}{2}} \\ & + N_6 \frac{\frac{N_9^2}{T^2} \exp\left(\frac{N_9}{T}\right)}{\left(\exp\left(\frac{N_9}{T}\right) - 1\right)^2} + N_7 \frac{\frac{N_{10}^2}{T^2} \exp\left(\frac{N_{10}}{T}\right)}{\left(\exp\left(\frac{N_{10}}{T}\right) - 1\right)^2} \\ & + \frac{2N_8}{3} \frac{\frac{N_{11}^2}{T^2} \exp\left(-\frac{N_{11}}{T}\right)}{\left(\frac{2}{3}\exp\left(-\frac{N_{11}}{T}\right) + 1\right)^2},\end{aligned} \tag{18}$$

with the scalar coefficients N_i for dry air (*ibid.*),

$$\begin{aligned} N_1 &= 3.490888032, & N_2 &= 2.395525583 \cdot 10^{-6}, \\ N_3 &= 7.172111248 \cdot 10^{-9}, & N_4 &= -3.115413101 \cdot 10^{-13}, \\ N_5 &= 0.223806688, & N_6 &= 0.791309509, \\ N_7 &= 0.212236768, & N_8 &= 0.197938904, \\ N_9 &= 3364.011, & N_{10} &= 2242.45, \\ N_{11} &= 11580.4, \end{aligned} \tag{19}$$

which is specified as valid for temperatures from 60 K to 2000 K.

The parameterisation (18) provides the isobaric specific heat capacity of dry air, considered as a mixture of ideal gases. This represents a more rigorous and accurate behaviour than assuming it to be a constant.

https://doi.org/10.5194/acp-2020-361
Preprint. Discussion started: 4 May 2020

Atmospheric Chemistry and Physics Discussions

4.3 The parameterisation of $c_p^0(T)$ from an engineer's perspective

The parameterisation from Dixon (2007) is not explicitly described to be based on particular assumptions or data sets. The author indicates his suggested parameterisation to hold within $0.1\,\%$ for temperatures between $200\,\mathrm{K}$ and $450\,\mathrm{K}$. For elevated air temperatures, the deviation between the ideal-gas limit $c_p^0(T)$ (Lemmon et al., 2000) and Dixon's parameterisation substantially increases. This is most likely due to the chosen type of polynomial approximation (Dixon, 2007), which increasingly departs from the reference $c_p^0(T)$ for gas temperatures exceeding $450\,\mathrm{K}$.

Concerning the thermophysical properties of humid air, the study by Tsilingiris (2008) provides further insight. Its purpose was to evaluate the transport properties as a function of different levels of the relative humidity and as a function of temperature (from $273\,\mathrm{K}$ to $373\,\mathrm{K}$) for the gas mixture of air with water vapour at a constant pressure ($1013\,\mathrm{hPa}$). The atmospherically relevant pressure range below $1013\,\mathrm{hPa}$ and temperatures smaller than $273\,\mathrm{K}$ were not considered. Although this study focused on providing a comprehensive account of moisture within air, mainly for technical purposes and engineering calculations, the possible usefulness of these findings to atmospheric investigations is also apparent. However, the impact of water vapour on the resulting gas mixture's $c_p(T)$ is significantly larger (cf. Tsilingiris, 2008) than the uncertainty of dry air's $c_p(T)$ that is discussed in the present work. Furthermore, the consideration of water vapour as a component of air requires very individual and case-specific computations of $c_p(T)$ of moist air, as water vapour is among the most variable constituents of the atmosphere.

The effort required to produce an analytical formulation for gas properties which best reflects the true gas behaviour may indicate that for engineering purposes (pneumatic shock absorbers, engines' combustion efficiency, improvements of turbofan/-prop propulsion, aerodynamics, material sciences, etc.), especially where pressures exceed atmospheric, the assumption of ideal-gas behaviour introduces excessive uncertainty.

5 The $\theta_{c_p(T)}$ from the temperature-dependent specific heat capacity of air

Previously introduced approaches for computing the specific heat capacity of dry air call for a brief discussion on how to use the obtained $c_p(T)$ to derive the potential temperature. In the following, $\theta_{c_p(T)}$ denotes the derived potential temperature that accounts for the temperature dependence of dry air's specific heat capacity. Furthermore, it should be noted that simply substituting any $c_p(T)$ value into the conventionally used and defining equation (13) for θ_{c_p} (WMO, 1966) may appear seductive but definitely leads to results inconsistent with $\theta_{c_p(T)}$ that is based on the reference parameterisation of dry air's $c_p(T)$. Therefore, the thermodynamically consistent use of $c_p(T)$ in the derivation of θ is described in the following.

5.1 Derivation of $\theta_{c_p(T)}$ based on the temperature-dependent specific heat capacity of dry air

In the derivation of the potential temperature (cf. Section 2), we note that, until reaching the expression for isentropic changes of state (9), no specific assumption was made about the specific heat capacity. As soon as the temperature dependence of the specific heat capacity comes into play, the re-assessment of (9) leads to

$$\frac{c_p(T)}{T}\,\mathrm{d}T = R_a \frac{\mathrm{d}p}{p}. \tag{20}$$

https://doi.org/10.5194/acp-2020-361
Preprint. Discussion started: 4 May 2020

Atmospheric Chemistry and Physics Discussions

Integration of (20) from the basic state $(p_0, \theta_{c_p(T)})$ to any other state (p, T) yields

$$R_a \ln\left(\frac{p}{p_0}\right) = \int_{p_0}^{p} \frac{\mathrm{d}p'}{p'} = \int_{\theta_{c_p(T)}}^{T} \frac{c_p(z)}{z}\,\mathrm{d}z, \tag{21}$$

where $\theta_{c_p(T)}$ is the desired potential temperature.

The rearrangement of (21) makes evident that the desired potential temperature is a zero of the function $F(x)$, given by

$$F(x) = \int_{x}^{T} \frac{c_p(z)}{z}\,\mathrm{d}z - R_a \ln\left(\frac{p}{p_0}\right). \tag{22}$$

To arrive at the desired potential temperature $\theta_{c_p(T)}$ for any given temperature and pressure, the equation $0 = F(x)$ must be solved for the variable x, which is the desired $\theta_{c_p(T)}$. Equation (22) has at most only one real zero, since its integrand is strictly positive which means $F(x)$ is strictly monotonic.

In the following, the ideal-gas reference potential temperature θ_{ref} is introduced, based on the formulation of the ideal-gas limit of dry air's specific heat capacity $c_p^0(T)$ in accordance with (18) as formulated by Lemmon et al. (2000). This reference potential temperature θ_{ref} represents the zero of $F(x)$ in (22), wherein $c_p(z)$ is to be replaced by $c_p^0(T)$.

It may be noted that further variants of a reference potential temperature are derivable by replacing $c_p(z)$ in (22) by any other expression of the specific heat capacity of air which may appear sufficiently accurate. The steps to compute or approximate the zero of the function (22), described in this study, are independent of the chosen heat capacity formulation.

Unfortunately, for a straightforward solution of the integral (22), the suggested parameterisation of c_p is too complex and an analytically insolvable nonlinear equation $0 = F(x)$ could result. Thus, an approximation of the equation's desired zero is required. Newton's method (cf., e.g., Deuflhard, 2011) provides a standard approach to numerically approximate the zero of a nonlinear equation. Proceeding from an initial guess x_0, Newton's method constructs a sequence $\{x_k\}_{k\in\mathbb{N}}$ defined by the recursion

$$\begin{aligned} x_{k+1} &= x_k - \frac{F(x_k)}{F'(x_k)} = x_k - \frac{F(x_k)}{-\frac{c_p(x_k)}{x_k}} \\ &= \frac{x_k}{c_p(x_k)}\left[c_p(x_k) + F(x_k)\right] \\ &= \frac{x_k}{c_p(x_k)}\left[c_p(x_k) - R_a \ln\left(\frac{p}{p_0}\right) + \int_{x_k}^{T} \frac{c_p(z)}{z}\,\mathrm{d}z\right]. \end{aligned} \tag{23}$$

The constructed sequence $\{x_k\}_{k\in\mathbb{N}}$ converges to the equation's desired zero. For the herein described computations, the iteration is stopped as soon as the absolute difference $|x_{k+1} - x_k|$ of two consecutive iterations falls below $10^{-8}\,\mathrm{K}$.

For the reference of air's specific heat capacity, $c_p^0(T)$, the integral (22) turns out not to be explicitly solvable. Therefore, with each iteration, the solution of the integral $\int_{x_k}^{T} \frac{c_p^0(z)}{z}\,\mathrm{d}z$ is approximated by subdividing the entire integration range, $[x_k, T]$, into intermediate intervals with respective size of at most $0.1\,\mathrm{K}$, and by applying Simpson's rule on each subinterval.

https://doi.org/10.5194/acp-2020-361
Preprint. Discussion started: 4 May 2020

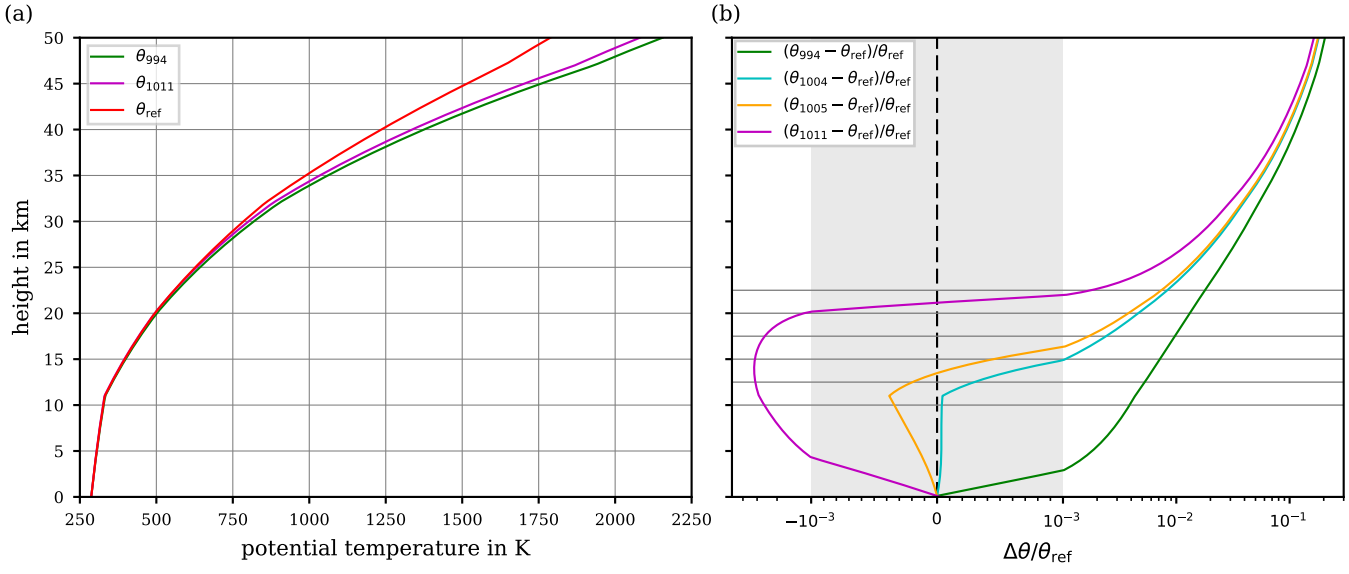

Figure 4. (a) Reference potential temperature θ_{ref} together with the potential temperatures θ_{994} and θ_{1011} relying on constant c_p values (e.g. 994 and 1011 $\mathrm{J\,kg^{-1}K^{-1}}$, cf. Table 1). (b) Relative differences $(\theta_{994}-\theta_{\mathrm{ref}})/\theta_{\mathrm{ref}}$ and $(\theta_{1011}-\theta_{\mathrm{ref}})/\theta_{\mathrm{ref}}$ between the reference potential temperature and potential temperatures relying on constant c_p values. For comparison, also the relative difference $(\theta_{1005}-\theta_{\mathrm{ref}})/\theta_{\mathrm{ref}}$ is displayed, for which $c_p = 1005\,\mathrm{J\,kg^{-1}K^{-1}}$ corresponds to the WMO recommendation. All profiles are based on the values for temperature and pressure according to the US Standard Atmosphere. Note the linear axis-scaling inside and the logarithmic scaling outside of the grey-shaded area in panel (b).

As a first guess x_0 for the Newton iteration, the conventional definition of θ_{c_p} based on a constant specific heat capacity (WMO, 1966) is inserted:

$$x_0 = T\left(\frac{p_0}{p}\right)^{\frac{R_a}{1005\,\mathrm{J\,kg^{-1}K^{-1}}}} = \theta_{1005}. \tag{24}$$

In the course of Newton's method, the sequence $\{x_k\}_{k\in\mathbb{N}}$ will converge to the unique zero for any initial guess x_0 due to the monotonicity of $F(x)$. However, the right choice of the initial guess x_0 substantially decreases the error of the first iteration x_1, speeding convergence to the desired zero of the function $F(x)$. Therefore, it may be comprehensible to use the conventional definition of θ_{c_p} as the first guess for the Newton iteration (23).

Solving the previously described root-finding problem by Newton's method over the comprehensive range of iteration steps (until the set requirement, i.e., $|x_{k+1}-x_k| < 10^{-8}\,\mathrm{K}$, is fulfilled) finally leads to the reference potential temperature θ_{ref}. This θ_{ref} is based on the ideal-gas limit of dry air's specific heat capacity $c_p^0(T)$, which refers to the current thermodynamic state-of-knowledge and, thus, we use θ_{ref} as our reference for the potential temperature in the following. For evaluating the results, the air temperature and pressure from the US Standard Atmosphere are used once more to set up the vertical profiles of the potential temperature. Figure 4a exhibits the resulting reference profile, i.e., θ_{ref}. Additionally, for comparison with the reference, further potential temperature profiles θ_{c_p} are shown based on two extremes of given constant values of air's specific heat capacity (cf.

https://doi.org/10.5194/acp-2020-361
Preprint. Discussion started: 4 May 2020

Atmospheric Chemistry and Physics Discussions

Table 1), $c_p = 994\,\mathrm{J\,kg^{-1}K^{-1}}$ and $c_p = 1011\,\mathrm{J\,kg^{-1}K^{-1}}$. Clearly, in particular at elevated altitudes, the courses of θ_{994} and θ_{1011} significantly deviate from the reference. To quantitatively evaluate the match between the different profiles, the relative difference of the four profiles, θ_{994}, θ_{1004}, θ_{1005} and θ_{1011}, with respect to the reference, i.e., $\Delta\theta/\theta_{\mathrm{ref}} = \left(\theta_{c_p} - \theta_{\mathrm{ref}}\right)/\theta_{\mathrm{ref}}$, is depicted in Figure 4b. The comparison impressively demonstrates that the θ_{c_p} profiles significantly depart from the reference by up to $\sim 250\,\mathrm{K}$ at $50\,\mathrm{km}$ altitude, corresponding to a relative difference of about $10\,\%$. With both extremes of constant c_p, the relative error level of $0.1\,\%$ is exceeded at altitudes below $5\,\mathrm{km}$. While θ_{994} continues to increasingly deviate from the reference, θ_{1011} re-enters and crosses the $0.1\,\%$ relative error interval (grey-shaded area) at altitudes between $\sim 20\,\mathrm{km}$ and $22.5\,\mathrm{km}$, before it reaches similar errors to the other θ_{c_p} profiles that are based on a constant c_p. Notably, up to an altitude of $15\,\mathrm{km}$, the reference potential temperature is comparably well matched by both the recommended θ_{1005} (WMO, 1966) and θ_{1004} (based on the frequently used alternative $c_p = 1004\,\mathrm{J\,kg^{-1}K^{-1}}$, cf. Table 1). Until $15\,\mathrm{km}$ altitude, both constant c_p values lead to errors of calculated θ_{c_p} which remain comparatively small within the $0.1\,\%$ relative error interval. However, above $\sim 17.5\,\mathrm{km}$, both θ_{1004} and θ_{1005} exceed the $0.1\,\%$ relative error interval, and further aloft their relative error with respect to the reference θ_{ref} increases rapidly.

In the context of numerical models of the atmosphere, the energy balance equation is occasionally formulated based on the potential temperature θ, thus θ constitutes a prognostic model variable. In such a case, the temperature T needs to be calculated from a given pair of values of pressure p and potential temperature θ. Using once more the defining equation (21), a zero of the function

$$0 = -\int_T^\theta \frac{c_p(z)}{z}\,\mathrm{d}z - R_a \ln\left(\frac{p}{p_0}\right) \tag{25}$$

is to be computed. Since (25) corresponds to the function F defined in (22) with the exception of a negative sign, the identical approximation procedure as outlined above in this section for the calculation of $(T, p) \mapsto \theta$ may be applied mutatis mutandis to calculate the transformation $(\theta, p) \mapsto T$.

In any case, a certain effort is required to implement the new formulation of the potential temperature in an atmospheric model, as this equation should be based on the implicit definition (21) and such a goal may be subject of future endeavours.

5.2 Approximations of the reference potential temperature

Of course, the previously described procedure to compute the potential temperature may appear to be anything but practical. Indeed, due to the complications inherent with:

- the requirement to numerically solve the integral in the function $F(x)$ and
- the need to use Newton's method for an iteration sequence to approach the zero of $F(x)$,

a convenient approach to re-assess the conventional definition of the potential temperature is not provided at all. This motivates the development of a more practical approximation of the reference potential temperature. To arrive at a practicable

https://doi.org/10.5194/acp-2020-361
Preprint. Discussion started: 4 May 2020

Atmospheric Chemistry and Physics Discussions

approximation procedure, the two principal steps in the suggested procedure are briefly outlined in the following, whereas the comprehensive details and intermediate derivation steps are found in Appendix C.

Proceeding from the definition (22) of the function $F(x)$, the computation of the integral $\int_x^T \frac{c_p^0(z)}{z}\,\mathrm{d}z$ becomes the first obstacle to a practical approximation. Therefore, a plausible initial step is to replace the integral by an expression that is easier to treat. This expression may be proposed as $f(T) - f(x)$, where the function f is defined as $f(x) = b_0 + b_1 \ln(x - b_2) + b_3 x + b_4 x^2$ and which is recognisable as an approximated primitive of $\frac{c_p^0(z)}{z}$, see Appendix C1. The choice of the functional form of f is motivated by the exact primitive of the integral in the case of a constant c_p.

As previously discussed (cf. Section 5.1), the formulation of a new expression for the potential temperature based on the temperature-dependent specific heat capacity $c_p(T)$ requires finding the zero of the equation $0 = F(x)$, where the function $F(x)$ is defined in (22). Replacing the exact integral in (22) by the difference $f(T) - f(x)$ means that $F(x)$ is substituted by the function

$$\widehat{F}(x) = f(T) - f(x) - R_a \ln\left(\frac{p}{p_0}\right). \tag{26}$$

Consequently, the resulting approximated reference potential temperature, i.e., the respective zero of the function $\widehat{F}(x)$, is denoted as $\theta_{\mathrm{ref}}^{\mathrm{approx}}$.

The difference between the approximation result and the reference, i.e.,

$$\theta_{\mathrm{ref}} - \theta_{\mathrm{ref}}^{\mathrm{approx}}, \tag{27}$$

is then referred to as the basic error of the approximation. Note that the replacement of the function F by $\widehat{F}$ only circumvents the integration in F; the root-finding problem $0 = \widehat{F}(x)$ for the approximated reference potential temperature $\theta_{\mathrm{ref}}^{\mathrm{approx}}$ remains analytically not solvable.

Therefore, the second move towards a practical approximation procedure is to construct approximations $\theta^{(k)}$ to the zero of $\widehat{F}(x)$ by using Newton's method, see Appendix C2. Newton's method is an iterative procedure; the notation $\theta^{(k)}$ refers to the k-th computed iterate. Hence, $\theta^{(k)}$ constitutes an approximation to $\theta_{\mathrm{ref}}^{\mathrm{approx}}$, and, in the limit $k \to \infty$, the approximation error

$$\theta_{\mathrm{ref}}^{\mathrm{approx}} - \theta^{(k)} \tag{28}$$

vanishes. Two formulations of Newton's method are distinguished in Appendix C2, i.e., the principal application of Newton's method, and its further derivative, called Householder's method. Both formulations require the stipulation of one of the iterates $\theta^{(k)}$ as sufficient to obtain a result of appropriate accuracy. The higher the number of iterations, of course, the smaller is the error (28), whereas the basic error (27) remains unaffected by the number of iterations. Hence, in any case, the basic error (27) is to be accepted as at least implied in the final approximation, even though a well-chosen $\theta^{(k)}$ could result in an approximation error $\theta_{\mathrm{ref}} - \theta^{(k)}$ that is smaller than the basic error.

The various errors implied in the proposed approximation procedure combining for the approximation's total error, as well as accompanying details, are discussed in Appendix D. In brief, Figure 5a illustrates the basic error (27) based on the pressure and temperature profiles of the US Standard Atmosphere, as these provide atmospherically meaningful averages of realistic

https://doi.org/10.5194/acp-2020-361
Preprint. Discussion started: 4 May 2020

Atmospheric Chemistry and Physics Discussions

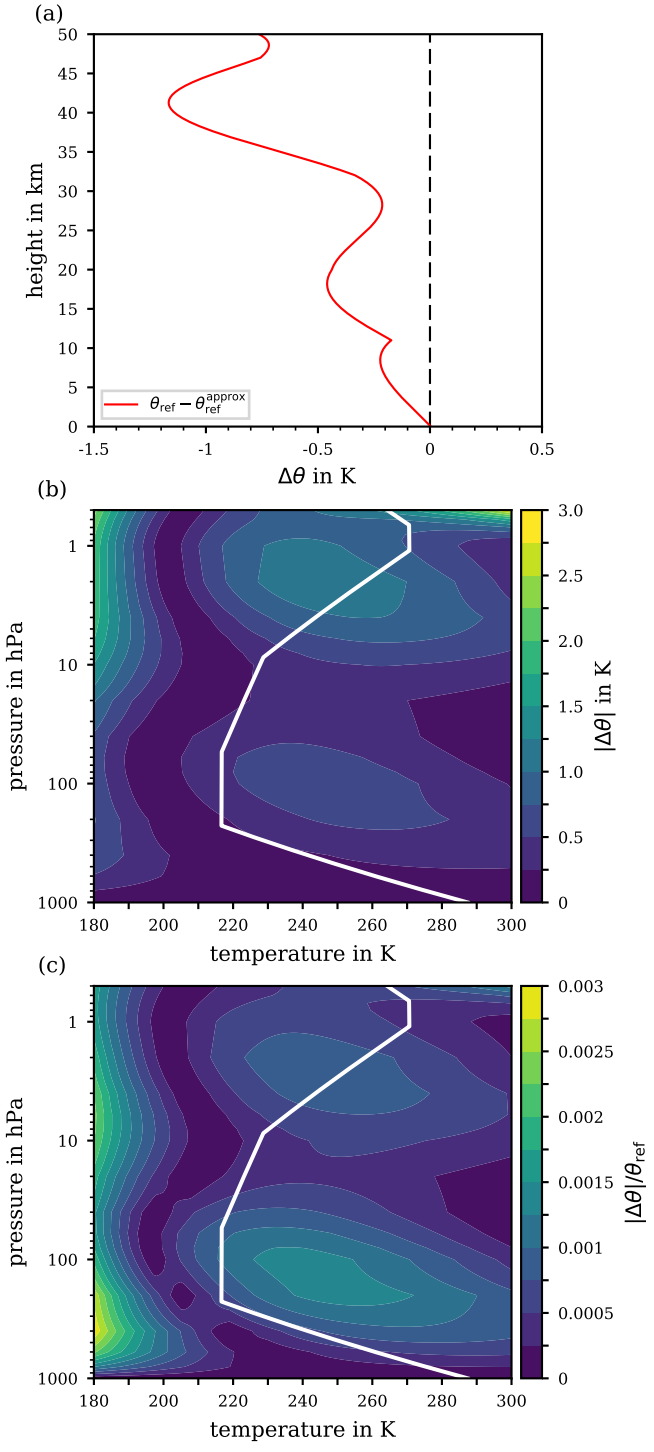

Figure 5. Absolute basic error $\Delta\theta = \theta_{\mathrm{ref}} - \theta_{\mathrm{ref}}^{\mathrm{approx}}$, cf. (27), from approximating the reference potential temperature along the US Standard Atmosphere (a) and for the extended pressure range $1000\,\mathrm{hPa}$ to $0.5\,\mathrm{hPa}$ and temperature range $180\,\mathrm{K}$ to $300\,\mathrm{K}$ (b). For orientation, the white solid line indicates the p-T-profile from the US Standard Atmosphere. The relative basic error $|\Delta\theta|/\theta_{\mathrm{ref}}$ is shown in panel (c) for the extended pressure and temperature range.

https://doi.org/10.5194/acp-2020-361
Preprint. Discussion started: 4 May 2020


Atmospheric Chemistry and Physics Discussions

temperature-pressure data pairs. Based on the parameters of the US Standard Atmosphere, the basic error inherent with the approximation remains below $1.25\,\mathrm{K}$ up to altitudes of $50\,\mathrm{km}$. Thus, regarding the subsequent iteration process, a substantial improvement of the error compared to $\sim 1.5\,\mathrm{K}$ is not to be expected for the total error of approximating the reference potential temperature.

An error analysis exclusively based on the US Standard Atmosphere is constrained to specific combinations of the air's pressure and temperature, potentially suppressing latent errors that may emerge if certain fluctuations of the real atmosphere's temperature and pressure profiles are considered. Thus, the error analysis is extended to an atmospheric pressure (p) and temperature (T) range, from $1000\,\mathrm{hPa}$ to $0.5\,\mathrm{hPa}$ and from $180\,\mathrm{K}$ to $300\,\mathrm{K}$, such that the conditions within the entire troposphere and stratosphere, including the stratopause, are covered. Figure 5b illustrates the absolute basic error (27) for the extended ranges of pressure and temperature while Figure 5c illustrates the relative basic error $|\theta_{\mathrm{ref}} - \theta_{\mathrm{ref}}^{\mathrm{approx}}|\,/\theta_{\mathrm{ref}}$. The contours in Figures 5b and 5c mainly highlight two regions: at $\sim 100\,\mathrm{hPa}$ where $\Delta\theta$ never rises above $0.75\,\mathrm{K}$ which corresponds to a maximum relative basic error of $0.15\,\%$, and in a pressure range from $\sim 5\,\mathrm{hPa}$ to $1\,\mathrm{hPa}$ where a $\Delta\theta$ of $1.25\,\mathrm{K}$ is never exceeded, corresponding to relative errors of at most $0.1\,\%$. Note that the entire $\Delta\theta$ scale ranges up to $3\,\mathrm{K}$, which may only be reached at pressures below $0.8\,\mathrm{hPa}$ combined with temperatures above $280\,\mathrm{K}$.

As previously discussed, the basic error is unavoidable and is to be accepted when applying the suggested substitution for the integral in the definition of the function $F(x)$ in (22). However, as outlined in Appendix C2, the second iterate $\theta^{(2)}$ of Newton's method (principal application), may thoroughly suffice for the final approximation to the reference potential temperature θ_{ref}, as this iteration level already features an approximation error (28) which is negligibly small. Figure 6a illustrates the total relative error of the suggested approximation $\theta^{(2)}$ with respect to the ultimate reference θ_{ref} for the extended ranges of pressure and temperature. Indeed, the contour pattern in Figure 6a and the basic relative approximation error shown in Figure 5c are remarkably similar. Thus, the iteration process itself imparts only a minor contribution to the total error compared to the basic approximation error.

The total approximation error, which is

$$\theta_{\mathrm{ref}} - \theta^{(2)} = (\theta_{\mathrm{ref}} - \theta_{\mathrm{ref}}^{\mathrm{approx}}) + \left(\theta_{\mathrm{ref}}^{\mathrm{approx}} - \theta^{(2)}\right), \tag{29}$$

is dominated by the unavoidable basic error (first bracket) and augmented by a negligible error inherent to the iteration (second bracket), also supporting the conclusion that the second iterate of Newton's method is an appropriate approximation procedure. Figure 7 presents step-wise instructions for the computation of the second iterate approximation to the reference potential temperature, and may serve as a guide to follow the numerous equations and intermediate analytical steps described throughout the derivations in Appendix C.

For completeness, Figures 6b and 6c exhibit a final comparison by means of the logarithmic difference and the logarithmic relative difference between the reference potential temperature θ_{ref} and the conventional definition θ_{c_p} (WMO, 1966) based on a constant specific heat capacity $c_p = 1005\,\mathrm{J\,kg^{-1}K^{-1}}$. Notably, over a wide altitude range within the troposphere (i.e., for atmospheric pressures greater than $\sim 100\,\mathrm{hPa}$), the absolute error $\Delta\theta = |\theta_{1005} - \theta_{\mathrm{ref}}|$ remains below $1\,\mathrm{K}$, cf. Figure 6b, corresponding to a relative error $\Delta\theta/\theta_{\mathrm{ref}}$ of at most $0.1\,\%$. However, in the pressure range below $\sim 100\,\mathrm{hPa}$, deviations of

https://doi.org/10.5194/acp-2020-361
Preprint. Discussion started: 4 May 2020

Atmospheric Chemistry and Physics Discussions

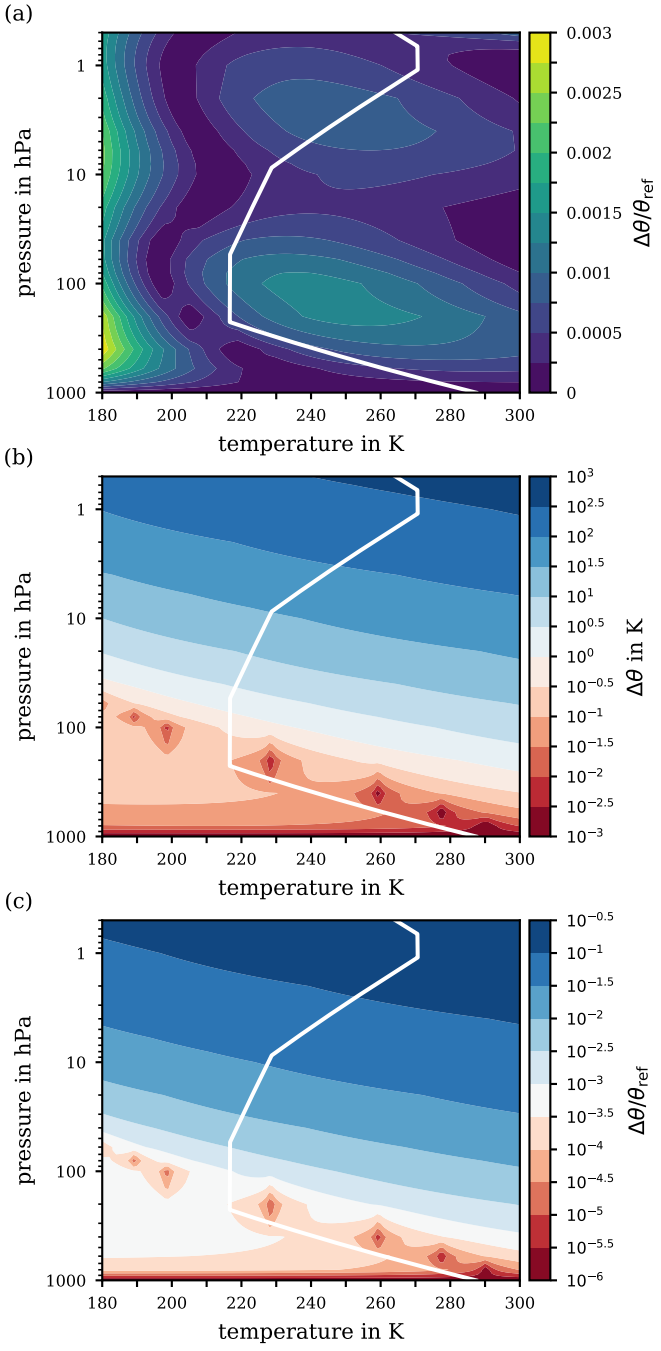

Figure 6. (a) Relative error $\Delta\theta/\theta_{\mathrm{ref}} = \left|\theta^{(2)} - \theta_{\mathrm{ref}}\right| / \theta_{\mathrm{ref}}$ of the second iterate $\theta^{(2)}$, obtained with Newton's method for the ranges of pressure and temperature from 1000 hPa to 0.5 hPa and from 180 K to 300 K, respectively. Panels (b) and (c) exhibit the difference $\Delta\theta = |\theta_{1005} - \theta_{\mathrm{ref}}|$ and relative difference $\Delta\theta/\theta_{\mathrm{ref}}$, respectively, on a logarithmic scale between the reference potential temperature θ_{ref} and the potential temperature θ_{1005} based on a constant specific heat capacity ($c_p = 1005\,\mathrm{J\,kg^{-1}K^{-1}}$). For orientation, the white solid line indicates the p-T-profile from the US Standard Atmosphere.

https://doi.org/10.5194/acp-2020-361
Preprint. Discussion started: 4 May 2020

Atmospheric Chemistry and Physics Discussions

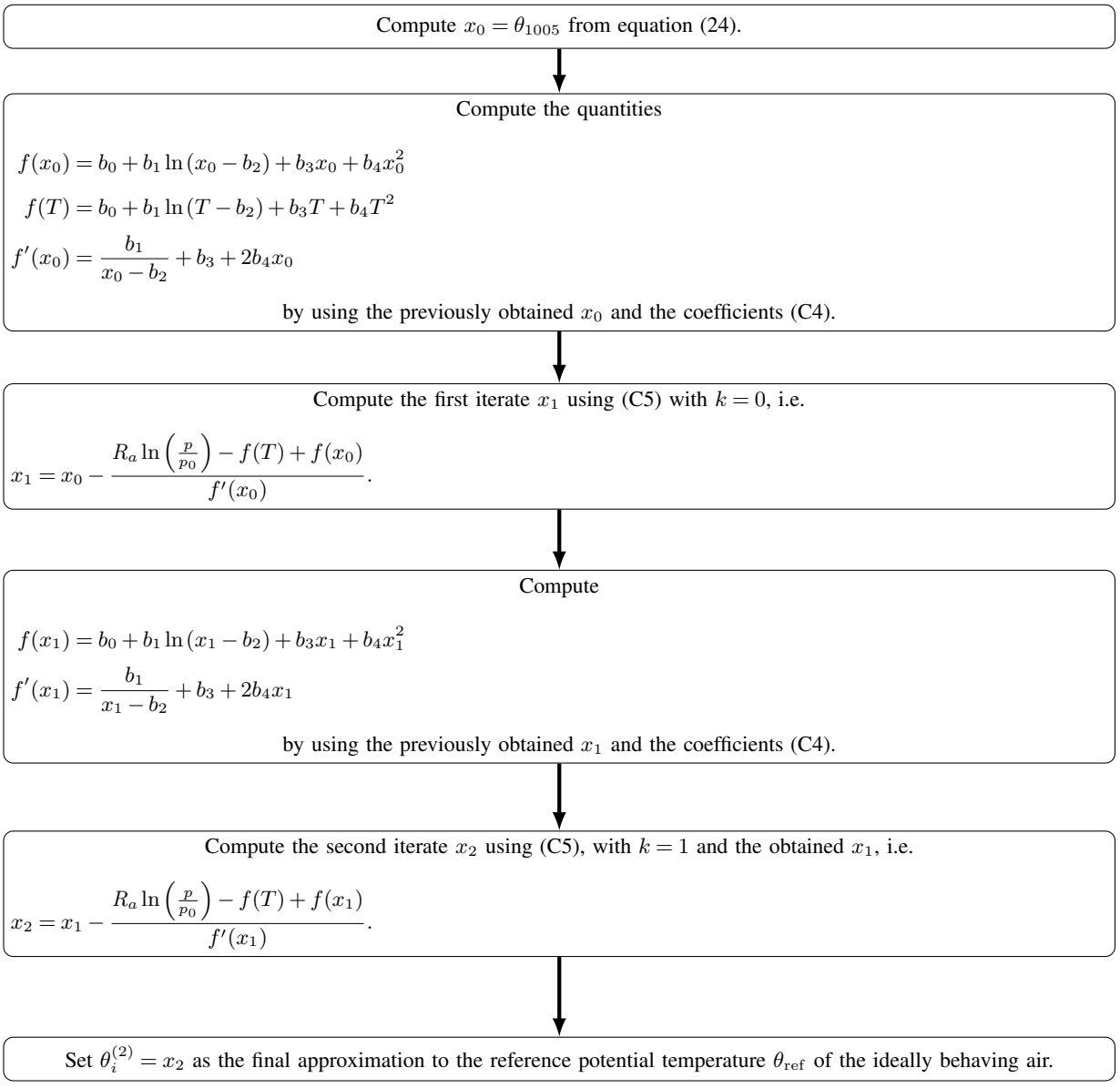

Figure 7. Flowchart guiding through the process of computing the approximation $\theta^{(2)}$ by using Newton's formulation (C5) until its second iteration, wherein T (in K) and p (in hPa) are the atmospheric air conditions in terms of temperature and pressure, respectively, and p_0 is set to 1000 hPa (WMO, 1966). Table C1 collects values of θ_{ref} and the approximation $\theta^{(2)}$ together with intermediate results for selected pairs of temperature and pressure to verify a computation according to this instruction.

https://doi.org/10.5194/acp-2020-361
Preprint. Discussion started: 4 May 2020


Atmospheric Chemistry and Physics Discussions

the real atmospheric conditions from those of the US Standard Atmosphere could increase the absolute error $\Delta\theta$ from a few K to up to 10 K, corresponding to an increase of the relative error to 1 %. Further critical pressure levels are at $\sim 20\,\mathrm{hPa}$ and $\sim 5\,\mathrm{hPa}$, where the error's magnitude increases to several tens and several hundreds of K, respectively. At a pressure of $0.5\,\mathrm{hPa}$, an absolute error $\Delta\theta$ of up to 500 K is reached, which corresponds to a relative error of 10 % or even more.

6 The potential temperature for air as a real gas

To calculate real-gas effects on the potential temperature, we use the model embedded in *REFPROP* (Lemmon et al., 2018), a standard reference database from NIST. This model treats air as a mixture and employs state-of-the art reference equations of state for pure nitrogen (Span et al., 2000), oxygen (Schmidt and Wagner, 1985), and argon (Tegeler et al., 1999). The mixing rule and binary interaction parameters are taken from the GERG-2008 model (Kunz and Wagner, 2012). From its definition in terms of an isentropic process, the potential temperature $\theta_{\mathrm{real}}(T, p)$ is defined implicitly by

$$s(\theta_{\mathrm{real}}, p_0) = s(T, p), \tag{30}$$

where s is the specific entropy. Calculating $\theta_{\mathrm{real}}(T, p)$ is a two-step process. First, the specific entropy s is computed at temperature T and pressure p. Then, the temperature θ_{real} is found that gives the same entropy s at the ground pressure p_0. This is an iterative calculation, but it is accomplished automatically within the *REFPROP* software (Lemmon et al., 2018).

One caveat should be mentioned regarding the computed potential temperatures. The range of validity of the equations of state for the air components (Span et al., 2000; Schmidt and Wagner, 1985; Tegeler et al., 1999) extends only up to 2000 K. At very high altitudes, computed values of θ_{real} exceed this limit. While all the equations extrapolate in a physically realistic way, their quantitative accuracy is less certain above 2000 K. This caveat also applies to the ideal-gas calculations; the correlations for $c_p^0(T)$ for N_2 and O_2 are extrapolations beyond 2000 K. However, since the same ideal-gas values are used in the real-gas calculations, any inaccuracy in $c_p^0(T)$ will cancel when evaluating the difference between ideal-gas and real-gas values of θ.

Figure 8 illustrates the comparison between the real-gas potential temperature θ_{real} and the ideal-gas reference potential temperature θ_{ref}. Figure 8a shows the difference $\theta_{\mathrm{real}} - \theta_{\mathrm{ref}}$, once more along the p-T-profile of the US Standard Atmosphere. Figure 8b accounts again for any p-T-combination of extended range but shows the relative difference instead. The difference between θ_{real} and θ_{ref} never exceeds 0.1 K for the absolute difference or $30 \cdot 10^{-5} = 0.03\,\%$ for the relative difference. As may be anticipated from the deviation of c_p^0 shown in Figure 3 at low temperatures both from the experimentally determined values (which may be inaccurate) as well as from the *REFPROP* data, the real-gas effect on the specific heat capacity of dry air tends to increase towards the coldest gas temperatures. However, the difference between the real- and ideal-gas approaches results in essentially no substantial difference between the resulting θ's, neither at ground conditions (for any temperature at $\sim 1000\,\mathrm{hPa}$) nor at very high altitudes (at pressures below $\sim 1\,\mathrm{hPa}$). While the negligible difference between θ_{real} and θ_{ref} near ground levels is less surprising, the diminished difference at higher altitudes reflects that in this region the potential temperature reaches such high values that the difference between the real-gas and the ideal-gas specific heat capacity becomes insignificant. Within the intermediate (stratospheric) region, the low pressures (and thus the low air densities) cause the ideal-gas assumption

https://doi.org/10.5194/acp-2020-361
Preprint. Discussion started: 4 May 2020

Atmospheric Chemistry and Physics Discussions

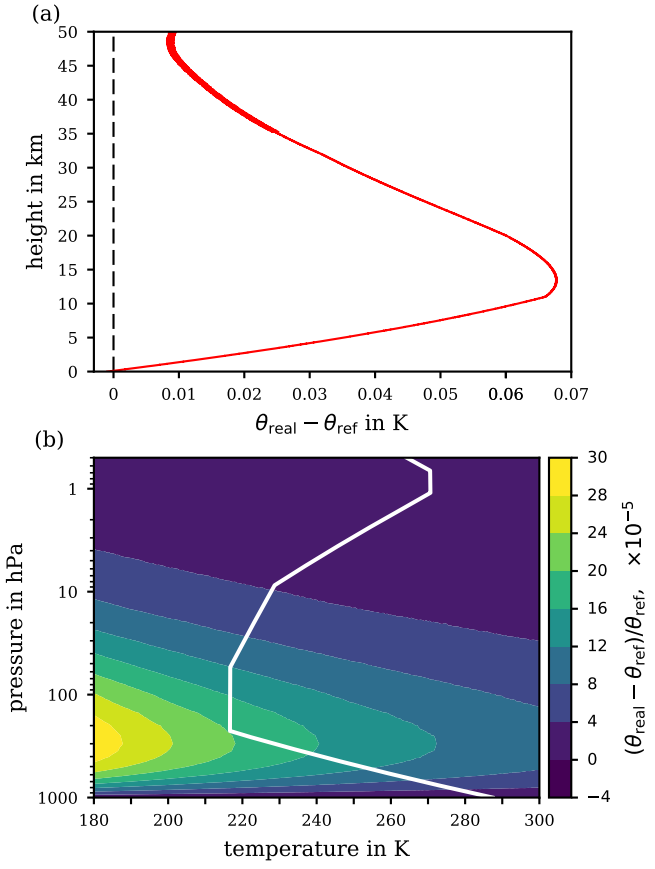

Figure 8. Difference $\theta_{\text{real}} - \theta_{\text{ref}}$ reflecting the deviation of the potential temperature θ_{real}, based on the properties of air behaving as a real gas under variable temperature and pressure, from the herein derived potential temperature expression θ_{ref} for the ideal-gas limit of the air's specific heat capacity $c_p^0(T)$. (a) Difference along the profile of the US Standard Atmosphere. (b) Relative difference in p-T-coordinates covering any combination of atmospherically relevant temperatures and pressures.

to be an accurate approximation even at low temperatures. In general, the degree to which a gas can be treated as an ideal gas is primarily a function of the (molar) density. For an ideal gas, the density is proportional to the quotient $\frac{p}{T}$; this is almost true also for real air. Hence, declining pressures together with rising temperatures both make the air's behaviour increasingly close to ideal.

7 Implications of the potential temperature on the prediction of gravity waves' breaking

As previously shown, the newly defined reference potential temperature θ_{ref} deviates most from the WMO-defined potential temperature θ_{1005} at high altitudes (cf. Figure 6). More particularly, not only do the values from both θ definitions differ, but also their vertical derivatives, i.e., $\frac{\partial \theta_{\text{ref}}}{\partial z}$ and $\frac{\partial \theta_{1005}}{\partial z}$. As the Brunt-Väisälä frequency N^2 depends on both the potential

https://doi.org/10.5194/acp-2020-361
Preprint. Discussion started: 4 May 2020

Atmospheric Chemistry and Physics Discussions

temperature and its vertical derivative, cf. (2), the resulting N^2, a measure of atmospheric stability, is affected by the definition of θ. This may have implications for the investigation of upward propagating gravity waves, which are emitted from the upper troposphere or lower stratosphere by various processes, e.g., spontaneous imbalance (Plougonven and Zhang, 2014), flow over mountains (Palmer et al., 1986), or convection (Choi and Chun, 2011). Various properties of gravity waves directly depend on the vertical profile of the Brunt-Väisälä frequency N^2. Specifically, the altitude of gravity wave breaking, if due to static instability, depends on N^2. To explore the implication of the θ definition on gravity wave breaking, vertical profiles of temperature and horizontal wind speed are used as shown in panels (a) and (b) of Figure 9. These are typical for mid latitudes for the months June and December, respectively, and they have been taken from the Upper Atmosphere Research Satellite Reference Atmosphere Project (URAP) data (Swinbank and Ortland, 2003).

Note that these profiles extend up to $85\,\mathrm{km}$, thus covering the entire stratosphere and most of the mesosphere, compared to the previously used vertical range reaching at most to $50\,\mathrm{km}$ (up to approximately stratopause level). Nevertheless, both the parameterised specific heat capacity of ideal-gas dry air (18) and the general derivation of the reference potential temperature (Section 5.1) are valid also at altitudes above $50\,\mathrm{km}$. Consequently, the new reference potential temperature also remains valid up to mesospheric altitudes, even though the approximate reference potential temperature $\theta_{\mathrm{ref}}^{\mathrm{approx}}$ may not match very well with θ_{ref} for altitudes above $50\,\mathrm{km}$.

Based on the temperature profiles in Figure 9a and considering the hydrostatic assumption as fulfilled, the Brunt-Väisälä frequencies are determined as

$$N^2_{\mathrm{ref}} = \frac{g}{\theta_{\mathrm{ref}}}\frac{\partial\theta_{\mathrm{ref}}}{\partial z} \quad \text{and} \quad N^2_{1005} = \frac{g}{\theta_{1005}}\frac{\partial\theta_{1005}}{\partial z}, \tag{31}$$

where $g = 9.81\,\mathrm{m\,s^{-2}}$ is the gravitational acceleration. The resulting vertical profiles of the Brunt-Väisälä frequencies are depicted in Figure 9c. Evidently, the values of N^2_{ref} and N^2_{1005} deviate from each other and, thus, lead to different predictions of the atmosphere's actual stability. Notably, the difference $N^2_{\mathrm{ref}} - N^2_{1005}$ increases with altitude as already implied by the increase of the difference $\theta_{\mathrm{ref}} - \theta_{1005}$ with altitude, shown in Figure 6b.

Following Lindzen (1981), static instability due to a gravity wave occurs whenever it can lead to an overturn of potential temperature, which is expressed as (e.g., Bölöni et al., 2016)

$$m(z)B(z) > N^2(z). \tag{32}$$

Here $m(z)$ is a gravity wave's vertical wave number at the altitude z, and $B(z)$ denotes the vertically varying buoyancy amplitude of the same wave. Thus, the (minimum) gravity wave breaking altitude $z_{\mathrm{b}} > z_0$ is predicted as the lowermost altitude where the condition $m(z_{\mathrm{b}})B(z_{\mathrm{b}}) = N^2(z_{\mathrm{b}})$ is satisfied.

To explore the implications of using the new reference potential temperature instead of the WMO-defined potential temperature on the predicted altitude of gravity wave breaking, a typical altitude of $z_0 = 17.5\,\mathrm{km}$ is chosen as the initiation level of a gravity wave with horizontal wave number $k(z_0) = \frac{2\pi}{\lambda_x}$ and vertical wave number $m(z_0) = \frac{2\pi}{\lambda_z}$. The initial buoyancy amplitude $B(z_0)$ is set to

$$B(z_0) = B_{\mathrm{fact}}\frac{N^2(z_0)}{m(z_0)}, \tag{33}$$

https://doi.org/10.5194/acp-2020-361
Preprint. Discussion started: 4 May 2020

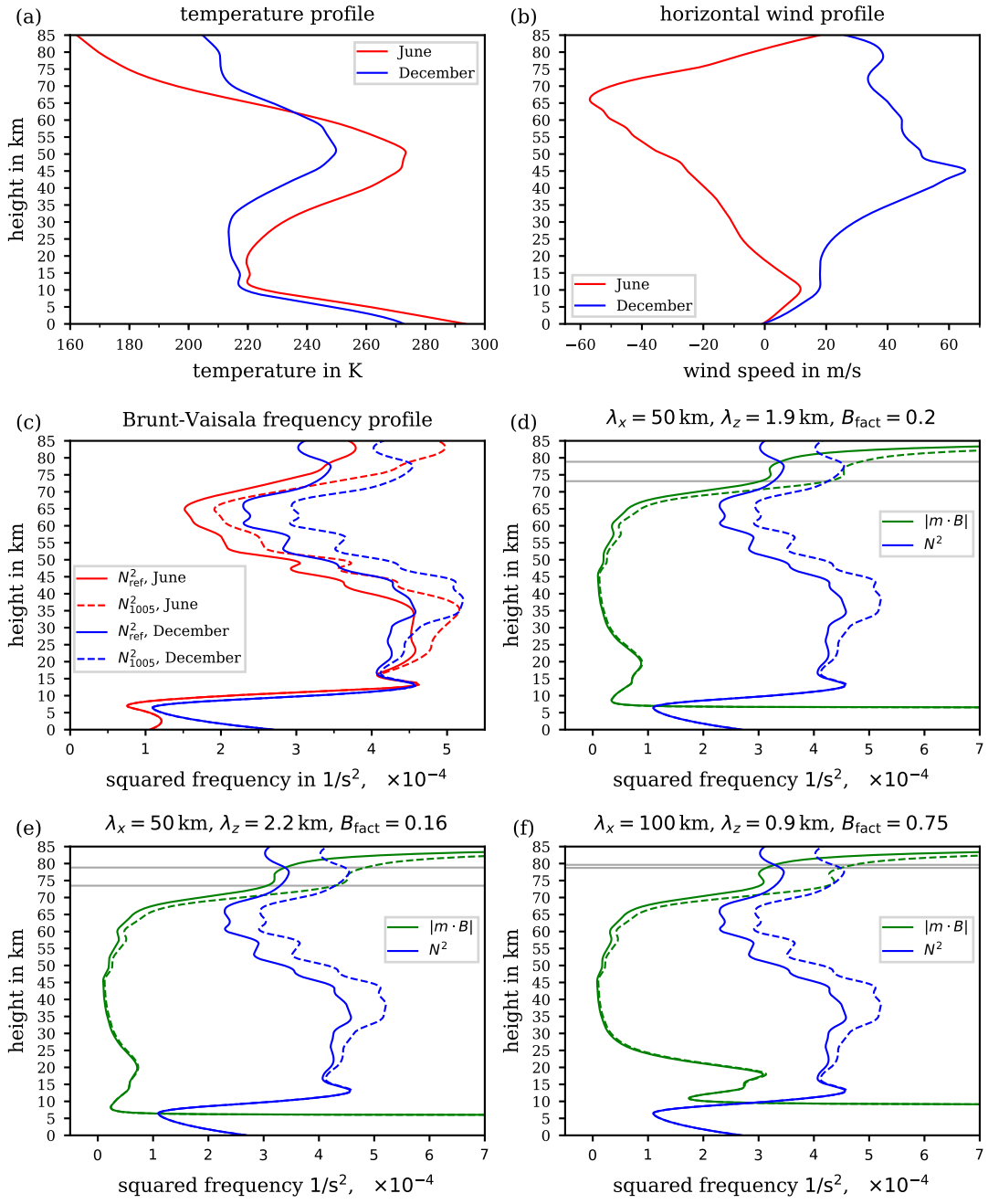

Figure 9. Vertical profiles of (a) temperature and (b) horizontal wind speed as typical for mid-latitudes in June and December, up to 85 km altitude. Resulting Brunt-Väisälä frequency N^2 (c), either based on θ_{ref} (solid lines) or on θ_{1005} (dashed lines). Panels (d), (e), and (f): vertical profiles of N^2_{ref} and N^2_{1005} for December (solid and dashed blue lines, respectively) with the modulus $|m(z) \cdot B(z)|$ (green lines), either based on θ_{ref} (solid lines) or on θ_{1005} (dashed lines), cf. text for further details. The panels' titles document the individually chosen values of the parameters λ_x, λ_z and B_{fact}. The thin grey horizontal lines indicate the altitude of the predicted wave breaking altitude, i.e. where $|m(z) \cdot B(z)|$ first coincides with $N^2(z)$ above the initiation height.

https://doi.org/10.5194/acp-2020-361
Preprint. Discussion started: 4 May 2020


Atmospheric Chemistry and Physics Discussions

with a scaling factor $0 < B_{\mathrm{fact}} < 1$ defining the wave amplitude at the initiation level with respect to static instability. The dependence of m and B on altitude is then determined by the classic steady-state approach as outlined, e.g., by Bölöni et al. (2016). The selected parameter values for the scaling factor B_{fact} are

$$B_{\mathrm{fact}} \in \{0.05, 0.06, 0.08, 0.1, 0.12, 0.14, 0.16, 0.18, \\ 0.2, 0.22, 0.24, 0.25, 0.3, 0.5, 0.75, 0.9\}, \tag{34}$$

while the selected horizontal wave lengths λ_x at initiation height are

$$\lambda_x \in \{\pm 100\,\mathrm{km}, \pm 50\,\mathrm{km}, \pm 10\,\mathrm{km}, \pm 5\,\mathrm{km}, \pm 1\,\mathrm{km}\}, \tag{35}$$

and the vertical wave length is varied between $100\,\mathrm{m}$ and $4000\,\mathrm{m}$ with $100\,\mathrm{m}$ increment. The aforementioned parameter values are used to compute the vertical profiles of $|mB|$ and N^2 based on the mid-latitude December profiles which are displayed in panels (d), (e), and (f) in Figure 9. The green lines illustrate the modulus $|mB|$ of the product of the vertical wave number and the buoyancy amplitude, while the blue lines exhibit the altitude dependence of the Brunt-Väisälä frequency N^2. The results shown as solid lines are based on the new reference potential temperature θ_{ref}; the results of the computations using θ_{1005} are represented by dashed lines. The predicted altitude of wave breaking is indicated by the first crossover of $|mB|$ and N^2 above the wave's initiation height, indicated by the thin grey horizontal lines. Apparently, the predicted altitudes of wave breaking differ by more than about $5\,\mathrm{km}$, depending on the definition of θ used (cf. panels (d), (e), (f) of Figure 9). Note that deviations of this scale are only found for the mid-latitude December vertical profiles of temperature and wind speed employed here, and hydrostatic gravity waves with initial horizontal wave lengths $\lambda_x \in \{100\,\mathrm{km}, 50\,\mathrm{km}\}$ and initial vertical wave lengths between approximately $1\,\mathrm{km}$ and $3\,\mathrm{km}$. Significant differences of predicted wave breaking altitudes were most frequently observed with initiation height amplitude scaling factors B_{fact} between 0.1 and 0.2, but larger values can also lead to significant differences, see Figure 9f. In essence, the improvement from the use of a more accurate potential temperature for predicting the altitude of gravity wave breaking is non-negligible, although not excessive. Nonetheless, these improvements may be of particular relevance for individual investigations, e.g., concerning the mesopause altitude, which involve specific vertical profiles at concrete atmospheric conditions and at locations other than the mid-latitudes. It needs to be emphasised, however, that predictions of the gravity wave breaking altitude are highly sensitive to variations along the vertical profiles of both the temperature and wind speed. Furthermore, the results of such predictions strongly depend on the chosen parameters at the gravity waves' initiation height.

8 Summary and Conclusions

Under the assumption that dry air is an ideal gas, a re-assessment of computing the potential temperature was introduced that accounts for the hitherto unconsidered temperature dependence of air's specific heat capacity. The new reference potential temperature θ_{ref} was introduced, which is thermodynamically consistent and based on a state-of-the-art parameterisation of the ideal-gas specific heat capacity of dry air from the National Institute of Standards and Technology (NIST). This reference

https://doi.org/10.5194/acp-2020-361
Preprint. Discussion started: 4 May 2020


Atmospheric Chemistry and Physics Discussions

potential temperature was compared to a potential temperature θ_{real} wherein the real-gas behaviour of dry air is considered. In the range of temperatures from $180\,\mathrm{K}$ to $300\,\mathrm{K}$ and the range of pressures from $1000\,\mathrm{hPa}$ to $0.5\,\mathrm{hPa}$, covering the atmospheric conditions of roughly the entire troposphere and stratosphere, the relative differences between θ_{ref} and θ_{real} are smaller than $0.03\,\%$ and may be considered negligible. Consequently, θ_{ref} even provides a reasonable approximation to the potential temperature of the real gas.

The difference between the newly derived reference potential temperature θ_{ref} and the conventionally determined potential temperature θ_{c_p} (with constant $c_p = 1005\,\mathrm{J\,kg^{-1}K^{-1}}$, as recommended by the World Meteorological Organisation, WMO, 1966) increases with altitude, e.g., $\Delta\theta \geq 1\,\mathrm{K}$ at pressures $p \leq 60\,\mathrm{hPa}$.

Derivation of a potential temperature that is consistent with thermodynamics and that accounts for the ideal-gas properties of dry air requires integration of Gibbs' equation and the subsequent solution of the resulting nonlinear equation. With a constant c_p, both analytical steps are straightforward, resulting in the conventional expression (13) as suggested by WMO (1966). However, if instead the temperature dependence of air's specific heat capacity $c_p(T)$ is considered, the integrals as well as the equations are not analytically solvable and, thus, the solution must be approximated. Both approximations were performed and described in detail. The integral was treated with the basic approximation and the solution of the nonlinear equation was approached by using the second iterate of Newton's method. As an alternative to Newton's classical method, a modified formulation of Householder's iteration method is provided, featuring accelerated convergence properties.

The suggested approximation steps to obtain a reference potential temperature have two main sources of error: the error $\theta_{\mathrm{ref}} - \theta_{\mathrm{ref}}^{\mathrm{approx}}$ inherent in the integral's basic approximation and the error $\theta_{\mathrm{ref}}^{\mathrm{approx}} - \theta^{(k)}$ of the k-th Newton iterate. The latter error approaches zero as $k \to \infty$, whereas the error resulting from the basic approximation remains well below $0.1\,\%$ (along the US Standard Atmosphere) for values of θ_{ref} of up to $\sim 2000\,\mathrm{K}$, hence up to stratopause altitudes. To keep this low error level also for $\theta_{\mathrm{ref}} > 2000\,\mathrm{K}$, the approximation may require an extension by means of a higher-order polynomial.

One of the foremost implications of the re-assessed potential temperature's definition concerns the use of θ as a vertical coordinate for the sorting, grouping, and comparison of (measured) data, e.g., along or across isentropes. Thereby, the re-assessed potential temperature constitutes a more accurate consideration of the air's actual properties. This particularly concerns, e.g., the specific heat capacity which is conventionally assumed as constant and for which various values are given depending on the textbook consulted.

Significant errors and biases may arise if, for instance, the conventional derivation of θ (WMO, 1966) is used together with values for air's specific gas constant (R_a) or air's specific heat capacity (c_p), which better comply with the most recent state-of-knowledge. Moreover, the use of the standard pressure $1013.25\,\mathrm{hPa}$ instead of $1000\,\mathrm{hPa}$ as defined by WMO (1966) and consistently used herein as ground level pressure (p_0), may cause an additional deviation of the resulting θ. Thus, the re-assessment of θ's definition could largely diminish such errors and biases and improve the comparability of data.

Concerning investigations of the propagation of gravity waves within the upper atmosphere, one further implication was investigated that arises from using the re-assessed potential temperature instead of the conventional definition. For predictions concerning the altitude of a gravity wave's breaking, the atmosphere's static stability is analysed, which is a function of both the potential temperature θ and its vertical derivative $\frac{\partial\theta}{\partial z}$. Using the re-assessed reference potential temperature instead of its

https://doi.org/10.5194/acp-2020-361
Preprint. Discussion started: 4 May 2020


Atmospheric Chemistry and Physics Discussions

conventional definition can result in a shift of predicted altitudes where the wave breaking occurs. The analysed cases revealed the prediction's high sensitivity to variations in the initiation conditions and the vertical profiles of temperature and wind. Moreover, the predictions concerning the presence of critical layers within the atmosphere may be impacted by using θ_{ref} instead of the conventional θ. Of all studied cases, a limited number of predictions produced a vertical deviation on the order of $5\,\mathrm{km}$. Of course, a comprehensive sensitivity study concerning these altitude predictions of gravity waves' breaking should be based on a larger variety of initiation parameters and vertical profiles of the temperature and wind fields from different geographical latitudes. However, such an investigation is beyond the scope of this study. The evaluation of the quantitative and/or qualitative significance of identified vertical shifts and deviations may be left to the reader.

On the one hand, such a re-assessment could take into account the current state of knowledge regarding the accuracy of thermodynamic variables and substance-related properties. On the other hand, this way the conceptional abstractness already inherent in θ is not further complicated by a misleading selection of parameters or reputed constants. There is no doubt that the conventional method is suitable for the description of most processes occurring within the troposphere. However, at stratospheric or even mesospheric altitudes, the neglect of the temperature dependence of the ideal-gas heat capacity in the convential definition increasingly distorts the resulting absolute values as well as the vertical course of the potential temperature. Ultimately, it seems obvious to profit from the computing capacities available today and from the known higher accuracy of physical variables and atmospheric parameters to carry out a reappraisal of the potential temperature, a useful (but not always consistently used) meteorological quantity.

Appendix A: Derivation of the specific heat capacity from thermodynamics

In the following, the derivation of the air's specific heat capacities C_V, C_p (capital letters indicate molar units) at constant volume and pressure, respectively, is summarised, mainly following the textbook exposition by Kondepudi and Prigogine (1998). We start with the ideal gas law

$$pV = NRT, \tag{A1}$$

with p the pressure, V the volume of the system, N the amount of gas within the volume, T the temperature, and R the universal gas constant. Additionally, the first law of thermodynamics is

$$\mathrm{d}U = \mathrm{d}Q - p\,\mathrm{d}V, \tag{A2}$$

with the internal energy U of the system and $\mathrm{d}Q$ specifies the change of heat. Insertion of the total derivative of the internal energy U in (A2), and assuming the system as thermodynamically closed, i.e., the molar amount N remains conserved ($\mathrm{d}N = 0$), leads to

$$\mathrm{d}Q - p\,\mathrm{d}V = \left.\frac{\partial U}{\partial T}\right|_{V,N} \mathrm{d}T + \left.\frac{\partial U}{\partial V}\right|_{T,N} \mathrm{d}V, \tag{A3}$$

https://doi.org/10.5194/acp-2020-361
Preprint. Discussion started: 4 May 2020

Atmospheric Chemistry and Physics Discussions

and subsequently

$$\mathrm{d}Q = \left.\frac{\partial U}{\partial T}\right|_{V,N} \mathrm{d}T + \left(p + \left.\frac{\partial U}{\partial V}\right|_{T,N}\right) \mathrm{d}V. \tag{A4}$$

If the system's volume is held constant, equation (A4) represents the definition of the constant-volume heat capacity C_V in molar units, i.e.,

$$\mathrm{d}Q = \left.\frac{\partial U}{\partial T}\right|_{V,N} \mathrm{d}T = C_V(p,T)\,\mathrm{d}T. \tag{A5}$$

Alternatively, assuming the system's pressure as constant, its volume is variable with total derivative

$$\mathrm{d}V = \left.\frac{\partial V}{\partial T}\right|_{p,N} \mathrm{d}T + \left.\frac{\partial V}{\partial p}\right|_{T,N} \underbrace{\mathrm{d}p}_{=0} = \left.\frac{\partial V}{\partial T}\right|_{p,N} \mathrm{d}T \tag{A6}$$

and, therefore, it results,

$$\begin{aligned}
\mathrm{d}Q &= \left.\frac{\partial U}{\partial T}\right|_{V,N} \mathrm{d}T + \left(p + \left.\frac{\partial U}{\partial V}\right|_{T,N}\right) \mathrm{d}V \\
&= \left.\frac{\partial U}{\partial T}\right|_{V,N} \mathrm{d}T + \left(p + \left.\frac{\partial U}{\partial V}\right|_{T,N}\right) \left(\left.\frac{\partial V}{\partial T}\right|_{p,N} \mathrm{d}T\right) \\
&= \left[\left.\frac{\partial U}{\partial T}\right|_{V,N} + \left(p + \left.\frac{\partial U}{\partial V}\right|_{T,N}\right) \left.\frac{\partial V}{\partial T}\right|_{p,N}\right] \mathrm{d}T \\
&= C_p(p,T)\,\mathrm{d}T,
\end{aligned} \tag{A7}$$

defining the isobaric molar heat capacity C_p. In general, this quantity depends on pressure as well as on temperature. However, if the gas is assumed as ideal, an important conclusion from the statistical description of an ideal gas is the fact that the internal energy U must be independent of the pressure (see, e.g., Fay, 1965).

Using this result, together with (A7) and the ideal gas law (A1), it follows

$$\begin{aligned}
C_p &= \left.\frac{\partial U}{\partial T}\right|_{V,N} + \left(p + \left.\frac{\partial U}{\partial V}\right|_{T,N}\right) \left.\frac{\partial V}{\partial T}\right|_{p,N} \\
&= \left.\frac{\partial U}{\partial T}\right|_{V,N} + p \left.\frac{\partial V}{\partial T}\right|_{p,N} \\
&= \left.\frac{\partial U}{\partial T}\right|_{V,N} + \left.\frac{\partial}{\partial T}(pV)\right|_{p,N} \\
&= \left.\frac{\partial U}{\partial T}\right|_{V,N} + \left.\frac{\partial}{\partial T}(NRT)\right|_{p,N} \\
&= \left.\frac{\partial U}{\partial T}\right|_{V,N} + NR.
\end{aligned} \tag{A8}$$

In the previous computations, there is no restriction on the temperature dependence of the internal energy $U(T)$. Therefore, even under the assumption of ideal-gas behaviour, the specific heat capacity C_p in (A8) is in general a function of temperature.

https://doi.org/10.5194/acp-2020-361
Preprint. Discussion started: 4 May 2020

Atmospheric Chemistry and Physics Discussions

Appendix B: Sensitivity of the conventional definition of θ to perturbations of c_p

This section explores, from a mathematical perspective, the sensitivity of the potential temperature formulation (13) based on a constant specific heat capacity. Considering the specific heat capacity c_p as a variable, the sensitivity of θ_{c_p} (13) to a small perturbation δ of c_p is described by the Taylor expansion

$$\begin{aligned}\theta_{c_p+\delta} &= \theta_{c_p} + \frac{\partial \theta_{c_p}}{\partial c_p}\delta + \mathcal{O}\left(\delta^2\right) \\ &= \theta_{c_p} - \theta_{c_p}\frac{R_a}{c_p^2}\ln\left(\frac{p_0}{p}\right)\delta + \mathcal{O}\left(\delta^2\right).\end{aligned} \tag{B1}$$

For any constant value of the specific heat capacity c_p and for a minor perturbation δ, the second summand within the expansion (B1) remains small for small values of $\ln\left(\frac{p_0}{p}\right)$. If the interval between the two pressure levels is very narrow, i.e., $p \approx p_0$, the expression $\ln\left(\frac{p_0}{p}\right)$ approximates $\ln(1) = 0$. Contrarily, if the pressure approaches very low values, i.e., $p \to 0\,\mathrm{Pa}$, the logarithmic expression diverges to negative infinity, i.e., $\ln\left(\frac{p_0}{p}\right) \to -\infty$, implying that the impact of the second summand intensifies with decreasing pressure, i.e., for increasing altitudes. Moreover, this may explain why the deviation between θ_{994} and θ_{1011}, as illustrated in Figure 2b, remains comparatively small within the troposphere and systematically increases with rising altitude, i.e., decreasing pressure levels.

Appendix C: Approximate computation of the reference potential temperature

This section summarises the detailed steps of approximating the function $F(x)$, defined in (22), by $\widehat{F}(x)$, defined in (26) (Section C1), as well as the approximations of the solutions of the resulting nonlinear equations by Newton's method (Section C2).

C1 Reformulating the function $F(x)$

Proceeding from the definition of a function $h(x)$

$$h(x) = \int_{T_1}^{x} \frac{c_p(z)}{z}\,\mathrm{d}z, \tag{C1}$$

with $T_1 = 180\,\mathrm{K}$, the function $F(x)$ may be rearranged as

$$\begin{aligned}F(x) &= \int_{x}^{T} \frac{c_p(z)}{z}\,\mathrm{d}z - R_a \ln\left(\frac{p}{p_0}\right) \\ &= h(T) - h(x) - R_a \ln\left(\frac{p}{p_0}\right).\end{aligned} \tag{C2}$$

The advantage of this reformulation of $F(x)$ is the inclusion of $h(x)$ which consists of an integral with fixed lower bound and a sole variable as upper bound. This way, the function $h(x)$ is numerically solvable, and subsequently $h(x)$ can be substituted

https://doi.org/10.5194/acp-2020-361
Preprint. Discussion started: 4 May 2020


Atmospheric Chemistry and Physics Discussions

by an approximation $f(x)$ that is defined as

$$f(x) = b_0 + b_1 \ln(x - b_2) + b_3 x + b_4 x^2. \tag{C3}$$

Notably, if c_p is constant, this function reduces to an exact primitive of the integrand $\frac{c_p}{z}$ with $b_3 = b_4 = 0$. Moreover, in this case, the resulting root-finding problem $0 = F(x)$ is exactly solvable and finally leads to the known conventional definition (13) of the potential temperature.

As a further step, the function $h(x)$ is numerically approximated, while $c_p(T)$ in (C1) is replaced by the ideal-gas limit of air's specific heat capacity $c_p^0(T)$. The integration interval $[T_1, x]$ with $T_1 \leq x \leq 2000\,\mathrm{K}$ is traversed in steps of at most $0.001\,\mathrm{K}$ while each step of the integration process is carefully approximated by using Simpson's rule.

By solving a least-squares problem, the coefficients in (C3) for the approximation of $h(x)$ by the function $f(x)$ are estimated as

$$\begin{aligned} b_0 &= -4072.2121328563667, \\ b_1 &= 797.09247926609601, \\ b_2 &= 29.587047521428016, \\ b_3 &= 0.41981158226925142, \\ b_4 &= -5.1008025097060311 \cdot 10^{-5}. \end{aligned} \tag{C4}$$

In Figure C1a the function $h(x)$ is graphed, together with the approximation $f(x)$, as well as the respective deviations $h(x) - f(x)$ in Figure C1b. Evidently, the absolute error inherent to the approximations is comparatively small as, over the entire temperature range above $190\,\mathrm{K}$, the approximation error never exceeds $\pm 1\,\mathrm{J\,kg^{-1}K^{-1}}$. Thus, the approximation error remains even smaller than the error caused by the scatter of given constant values of the specific heat capacity. Exclusively at temperatures below $190\,\mathrm{K}$, the approximation error rapidly rises above $1\,\mathrm{J\,kg^{-1}K^{-1}}$, bearing in mind that such absolute temperatures are only occasionally found in the atmosphere within a relatively narrow altitude interval at the cold point tropopause. Moreover, the deviation of $f(x)$ and $h(x)$ from each other appears negligible as the profiles almost ideally coincide (cf. Figure C1a).

C2 Finalised approximation of the reference potential temperature

As discussed in Section 5.1, the new formulation for the potential temperature based on the temperature-dependent specific heat capacity $c_p(T)$ requires solving the root-finding problem $0 = F(x)$, where the function $F(x)$ is defined in (22). However, since $F(x)$ contains an integral that complicates the root-finding process, this integral is substituted by the difference $f(T) - f(x)$, where f is given in Section C1. Therefore, $F(x)$ is replaced by the function $\widehat{F}(x)$ as defined in (26) and the zero of the equation $0 = \widehat{F}(x)$ is denoted as $\theta_{\mathrm{ref}}^{\mathrm{approx}}$.

https://doi.org/10.5194/acp-2020-361
Preprint. Discussion started: 4 May 2020

Atmospheric Chemistry and Physics Discussions

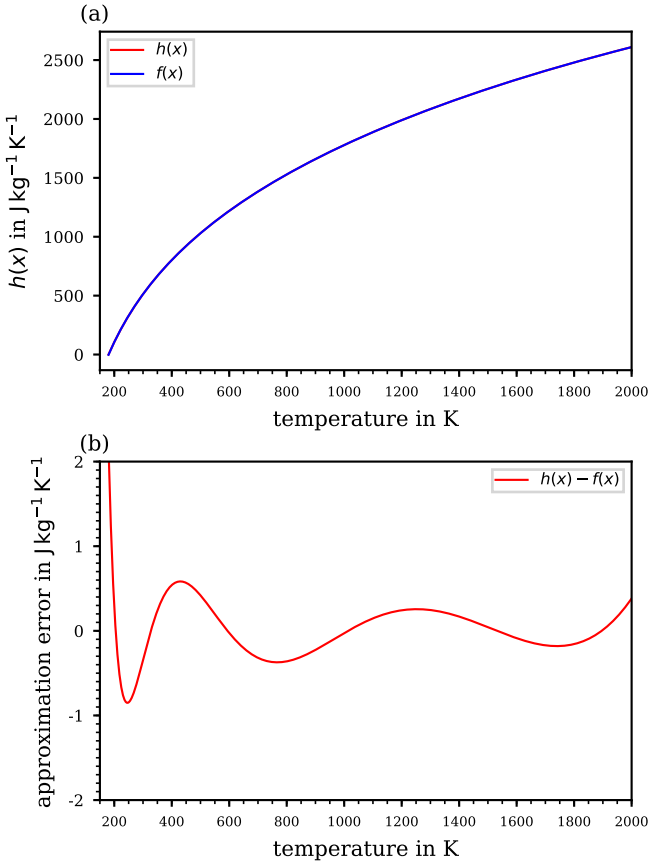

Figure C1. (a) Numerically evaluated function $h(x)$ together with its approximation $f(x)$; (b) the absolute approximation error $h(x) - f(x)$.

The equation $0 = \widehat{F}(x)$ is still not analytically solvable, so Newton's method is once more required. Using again $x_0 = \theta_{1005}$ as the initial guess, cf. (24), the iteration sequence for Newton's method is given by the recursion

$$\begin{aligned} x_{k+1} &= x_k - \frac{\widehat{F}(x_k)}{\widehat{F}'(x_k)} = x_k - \frac{f(T) - f(x_k) - R_a \ln\left(\frac{p}{p_0}\right)}{-f'(x_k)} \\ &= x_k - \frac{R_a \ln\left(\frac{p}{p_0}\right) - f(T) + f(x_k)}{f'(x_k)}. \end{aligned} \tag{C5}$$

https://doi.org/10.5194/acp-2020-361
Preprint. Discussion started: 4 May 2020


Atmospheric Chemistry and Physics Discussions

Instead of this standard formulation of Newton's method (C5), Householder's formulation

$$
\begin{aligned}
x_{k+1} &= x_k - \frac{\widehat{F}(x_k)}{\widehat{F}'(x_k)} - \frac{\widehat{F}''(x_k)}{2\widehat{F}'(x_k)} \left[\frac{\widehat{F}(x_k)}{\widehat{F}'(x_k)}\right]^2 \\
&= x_k - \frac{R_a \ln\left(\frac{p}{p_0}\right) - f(T) + f(x_k)}{f'(x_k)} \\
&\quad - \frac{f''(x_k)}{2f'(x_k)} \left[\frac{R_a \ln\left(\frac{p}{p_0}\right) - f(T) + f(x_k)}{f'(x_k)}\right]^2
\end{aligned}
\tag{C6}
$$

may be used, which allows for reducing the computation time due to its accelerated convergence speed. For completeness, the required derivatives f', f'' in the recursion formulas (C5) and (C6) are

$$
\begin{aligned}
f'(x) &= \frac{b_1}{x - b_2} + b_3 + 2b_4 x, \\
f''(x) &= 2b_4 - \frac{b_1}{(x - b_2)^2}.
\end{aligned}
\tag{C7}
$$

The final step on the way to formulate a new expression for the potential temperature requires defining one of the iterates x_k as appropriate enough for the approximations that result from applying the different methods:

- the standard of Newton's method (C5), simply referred to as Newton's method in the sequel, or
- Householder's method (C6).

While the mathematical expressions in (C5) and (C6) are of increasing complexity, the convergence rate of the approximating sequence increases with rising mathematical complication. The preferred method is determined by the accuracy required, i.e., an elevated accuracy level is necessarily associated with elevated computational effort for the approximation method. A discussion of the approximation errors is found in Appendix D.

Table C1 collects values of the new reference potential temperature θ_{ref}, together with the first two iterates $\theta^{(1)}$, $\theta^{(2)}$ using Newton's method (C5) and the first iterate $\theta^{(1)}_{\mathrm{Householder}}$ using Householder's method (C6) for five pairs of temperature and pressure along the US Standard Atmosphere, cf. Figure 1, which allows to verify a computation. The first height is chosen midway along the linearly decreasing temperature profile within the troposphere, while the other heights correspond to the kinks of the temperature profile.

Appendix D: Approximation error for the reference potential temperature

The following aims at a comprehensive investigation of the errors inherent with approximating the ultimate reference potential temperature θ_{ref}. As discussed in Section 5.2, the total error is a combination of the basic error $\theta_{\mathrm{ref}} - \theta^{\mathrm{approx}}_{\mathrm{ref}}$ and, furthermore, the approximation error that results from the approximation sequence $\theta^{\mathrm{approx}}_{\mathrm{ref}} - \theta^{(k)}$, where $\theta^{(k)}$ denotes the k-th iterate of the approximation sequence which is computed in accordance with either Newton's or Householder's method. The formulations of

https://doi.org/10.5194/acp-2020-361
Preprint. Discussion started: 4 May 2020

Atmospheric Chemistry and Physics Discussions

z in m	T in K	p in Pa	θ_{ref} in K	$\theta^{(1)}$ in K	$\theta^{(2)}$ in K	$\theta^{(1)}_{\mathrm{Householder}}$ in K
5500	252.4	50506.8	306.837	307.016	307.016	307.016
11000	216.65	22632.1	331.337	331.510	331.510	331.510
20000	216.65	5474.89	494.940	495.376	495.378	495.378
32000	228.65	868.019	855.324	855.172	855.656	855.660
47000	270.65	110.906	1637.052	1620.463	1637.726	1638.974

Table C1. Values of the new reference potential temperature θ_{ref} , together with the first two iterates $\theta^{(1)}$, $\theta^{(2)}$ using Newton's method and the first iterate $\theta^{(1)}_{\mathrm{Householder}}$ using Householder's method for five pairs of temperature and pressure along the US Standard Atmosphere. The computed values are rounded to three digits.

Newton's (C5) and Householder's (C6) method require replacing the function $F(x)$ by $\widehat{F}(x)$, and the approximation sequences $\theta^{(k)}$ converge to $\theta^{\mathrm{approx}}_{\mathrm{ref}}$ for $k \to \infty$. Consequently, the approximation error $\theta^{\mathrm{approx}}_{\mathrm{ref}} - \theta^{(k)}$ tends to zero for $k \to \infty$.

The analysis of the approximation error is initially based on the pressure and temperature profiles of the US Standard Atmosphere. Figure D1 shows the total relative errors $\left(\theta_{\mathrm{ref}} - \theta^{(1)}\right)/\theta_{\mathrm{ref}}$ of the first iterate (Figure D1a) and $\left(\theta_{\mathrm{ref}} - \theta^{(2)}\right)/\theta_{\mathrm{ref}}$ of the second iterate (Figure D1b), computed with Newton's or Householder's method. The first iterate still causes the approximation to have significant errors, especially at altitudes above $35\,\mathrm{km}$. However, the second iterate with either Newton's or Householder's method yields results with negligible approximation error. Hence, the total error of the approximation procedure is dominated by the unavoidable basic error, and may be deduced from the provided figures whenever the total error profile nearly congruently follows the profile of the basic error (cf. Figures D1b and 5a).

It may be noted that Householder's method achieves a significantly lower error level than Newton's method due to its accelerated rate of convergence. Compared to the first iterate approximations, computation up to the second iterate (cf. Figure D1b) achieves, in general, a considerable improvement for both methods, and both second iterate approximations approach the basic error quite closely (cf. Figure D1b). As is also evident from Figure D1b, compared to Householder's method, the second iterate with Newton's method results in a smaller total relative error $\left(\theta_{\mathrm{ref}} - \theta^{(2)}\right)/\theta_{\mathrm{ref}}$ relative to the ultimate reference potential temperature (indicated by a smaller distance to the dashed zero-line above $45\,\mathrm{km}$ altitude). Nevertheless, the relative approximation error, $\left(\theta^{\mathrm{approx}}_{\mathrm{ref}} - \theta^{(2)}\right)/\theta_{\mathrm{ref}}$, is larger compared to the second iterate with Householder's method. So, luckily, the second iterate with Newton's method provides a better approach to the reference potential temperature than that with Householder's method.

As for the discussion of the basic error in Section 5.2, the analysis of the total error should include all possible combinations of pressure and temperature in order to take into account fluctuations in the real atmosphere that deviate from the profile of the US Standard Atmosphere. Therefore, the extended analysis of the approximation error is summarised in Figure D2. The upper panels illustrate the total relative error of the second iterate for Newton's (Figure D2a) and Householder's method (Figure D2b). As previously shown, any further iteration with either method does not improve the approximation quality. The contour patterns in these panels show a remarkable similarity to the contours for the relative error of the basic approximation in Figure 5c. Also here (upper panels of Figure D2), two regions are highlighted by the contours, i.e., at $\sim 100\,\mathrm{hPa}$ and in a pressure

https://doi.org/10.5194/acp-2020-361
Preprint. Discussion started: 4 May 2020

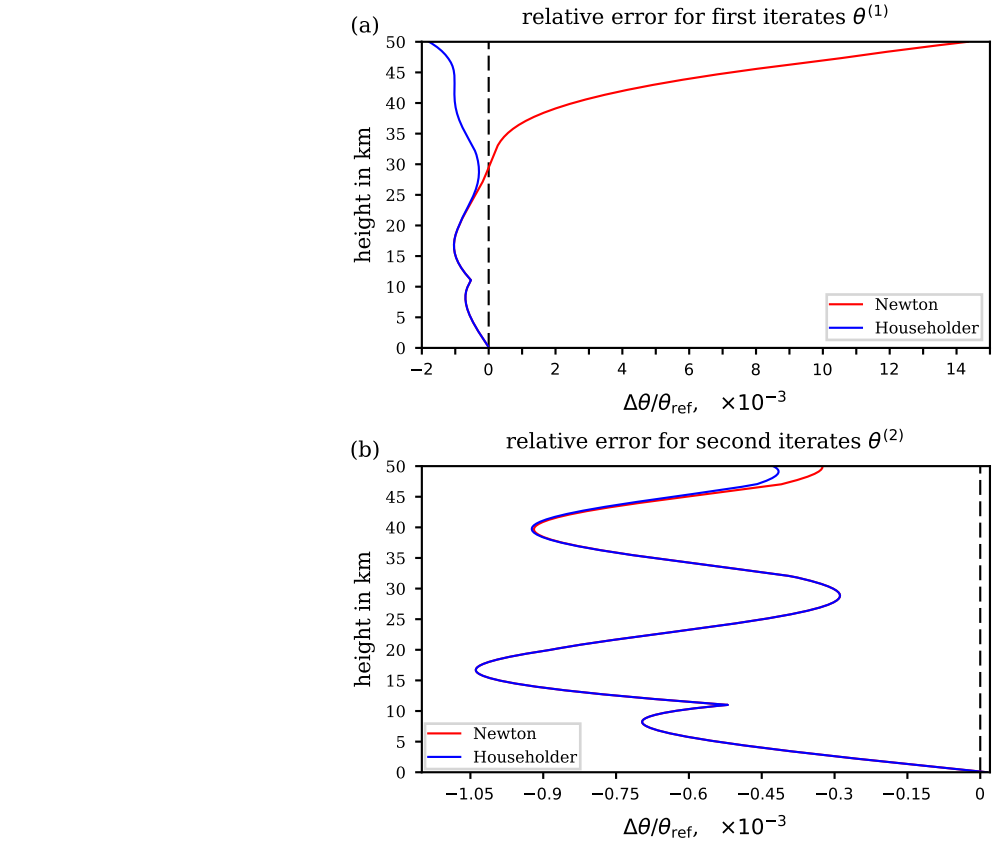

Figure D1. Total relative error along the US Standard Atmosphere arising from the iteration process by declaring (a) the first iterate $\theta^{(1)}$ or (b) the second iterate $\theta^{(2)}$ as the final approximation to the reference potential temperature θ_{ref}. Red curves: iterates computed using Newton's method (C5); blue curves: iterates computed using Householder's method (C6). Note the different range of the abscissae.

range from $\sim 5\,\mathrm{hPa}$ to $1\,\mathrm{hPa}$, featuring the same impact on $\Delta\theta/\theta_{\mathrm{ref}}$ of identical strength as the basic error. This result may not be surprising, since the second iteration step with both methods, Newton's and Householder's, was already proven to approach the approximation comparatively well, without worsening the total error level (cf. Figure D1b).

Consequently, concerning the required number of iterations and the method to use, the second iteration of Newton's method can be recommended to deliver appropriate results, with a relative error of less than $0.3\,\%$, up to the stratopause level ($\sim 50\,\mathrm{km}$). Householder's method features an accelerated convergence rate, and its use up to its first iterate $\theta^{(1)}$ may be already appropriate for certain applications. According to the total error of Householder's method up to its first iterate $\theta^{(1)}$ (Figure D2c), the resulting relative error remains below $7\,\%$ to a pressure level of $\sim 50\,\mathrm{hPa}$ and $\Delta\theta$ stays below $0.3\,\%$ to pressures of $\sim 2\,\mathrm{hPa}$. Thus, Figure D2 may serve as guidance to decide how many iterations with one or the other method best meets the individual accuracy requirements.

https://doi.org/10.5194/acp-2020-361
Preprint. Discussion started: 4 May 2020

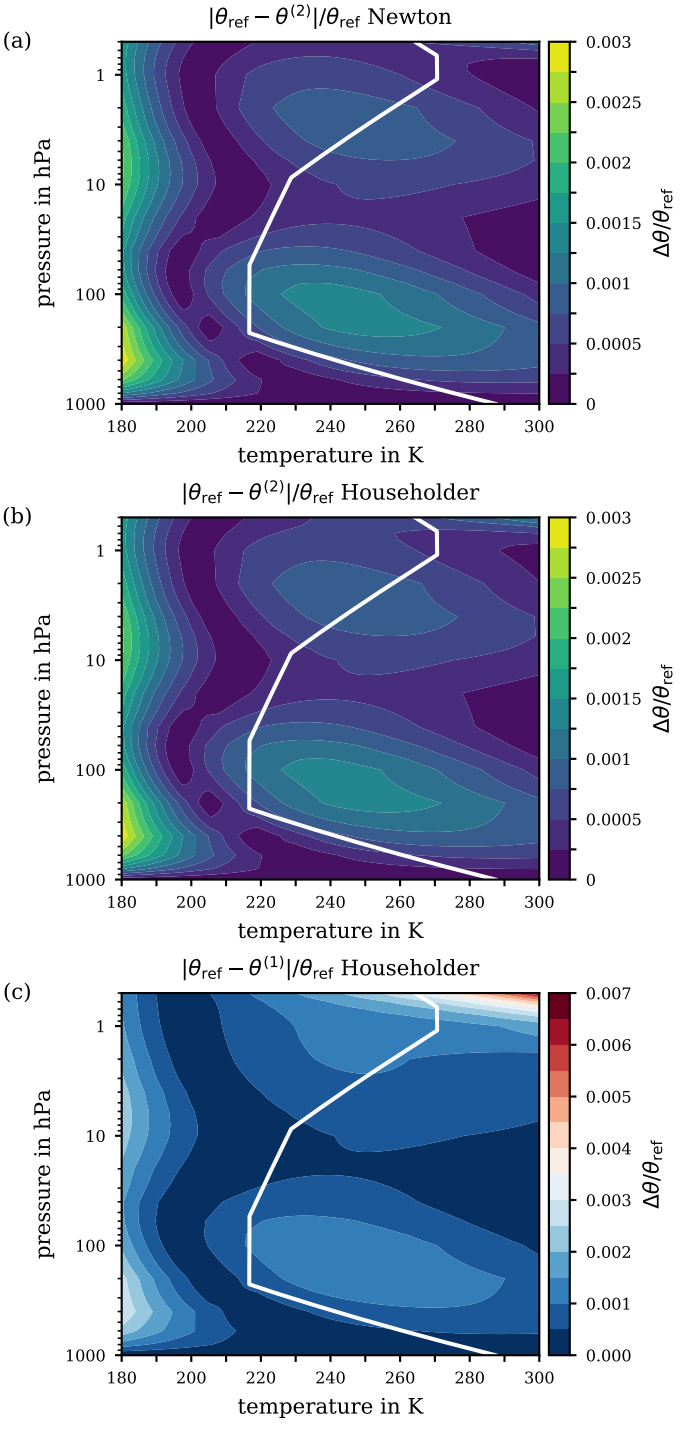

Figure D2. Relative error of the second iterates $\theta^{(2)}$ with (a) Newton's method and (b) Householder's method for the the ranges of pressure and temperature from 1000 hPa to 0.5 hPa and from 180 K to 300 K, respectively. (c) The absolute error arising from the first iterate $\theta^{(1)}$ with Householder's method. The white solid line indicates the p-T-profile from the US Standard Atmosphere. Note the different ranges of the $\Delta\theta$ scales.

https://doi.org/10.5194/acp-2020-361
Preprint. Discussion started: 4 May 2020

Atmospheric Chemistry and Physics Discussions

Author contributions. MB, RW, and PS conceived, designed, and carried out the main part of the research. UA contributed the implications on gravity wave breaking. AH gave advice about the heat capacity and performed the calculations of real-gas potential temperatures. MB and RW wrote the manuscript with contributions and reviews from all authors.

Competing interests. The authors declare that they have no conflict of interest.

Acknowledgements. We thank Eric W. Lemmon for his advice on the equation of state of dry air, Vera Bense for fruitful discussions on gravity wave breaking, Gergely Bölöni for providing us the vertical profiles in Section 7, and Miklós Szakáll for the hint concerning Titan's atmosphere. Manuel Baumgartner and Peter Spichtinger acknowledge support by the Deutsche Forschungsgemeinschaft (DFG) within the Transregional Collaborative Research Centre TRR165 Waves to Weather, (www.wavestoweather.de), projects B7 and Z2. Ralf Weigel received financial support by the *Bundesministerium für Bildung und Forschung* (BMBF) under the joint ROMIC-project *SPITFIRE* (01LG1205A). Ulrich Achatz and Peter Spichtinger acknowledge partial support by the DFG through the research unit Multiscale Dynamics of Gravity Waves (MS-GWaves) and through grants AC 71/12-2 and SP 1163/5-2.

https://doi.org/10.5194/acp-2020-361
Preprint. Discussion started: 4 May 2020

Atmospheric Chemistry and Physics Discussions

References

Awano, S.: JS-Diagrams for Air, Report of Aeronautical Research Institute, Tokyo Imperial University, 11, https://doi.org/10.1175/1520-0469(1970)027<0919:TDOICI>2.0.CO;2, https://repository.exst.jaxa.jp/dspace/handle/a-is/12312, 1936.

Bohren, C., Albrecht, B., and Albrecht, P.: Atmospheric Thermodynamics, Oxford University Press, https://books.google.de/books?id=SSJJ_RWJGe8C, 1998.

Bölöni, G., Ribstein, B., Muraschko, J., Sgoff, C., Wei, J., and Achatz, U.: The Interaction between Atmospheric Gravity Waves and Large-Scale Flows: An Efficient Description beyond the Nonacceleration Paradigm, Journal of the Atmospheric Sciences, 73, 4833–4852, https://doi.org/10.1175/JAS-D-16-0069.1, https://doi.org/10.1175/JAS-D-16-0069.1, 2016.

Bolton, D.: The Computation of Equivalent Potential Temperature, Monthly Weather Review, 108, 1046–1053, https://doi.org/10.1175/1520-0493(1980)108<1046:TCOEPT>2.0.CO;2, https://doi.org/10.1175/1520-0493(1980)108<1046:TCOEPT>2.0.CO;2, 1980.

Brasseur, G. P. and Solomon, S.: Aeronomy of the Middle Atmosphere, Springer, https://doi.org/10.1007/1-4020-3824-0, https://books.google.de/books?id=tZEpAQAAMAAJ, 2005.

Bücker, D., Span, R., and Wagner, W.: Thermodynamic Property Models for Moist Air and Combustion Gases, Journal of Engineering for Gas Turbines and Power, 125, 374–384, https://doi.org/10.1115/1.1520154, http://dx.doi.org/10.1115/1.1520154, 2002.

Catling, D. C.: 10.13 - Planetary Atmospheres, in: Treatise on Geophysics (Second Edition), edited by Schubert, G., pp. 429 – 472, Elsevier, Oxford, second edition edn., https://doi.org/10.1016/B978-0-444-53802-4.00185-8, http://www.sciencedirect.com/science/article/pii/B9780444538024001858, 2015.

Choi, H.-J. and Chun, H.-Y.: Momentum Flux Spectrum of Convective Gravity Waves. Part I: An Update of a Parameterization Using Mesoscale Simulations, J. Atmos. Sci., 68, 739–759, https://doi.org/10.1175/2010JAS3552.1, 2011.

Cotton, W. R., Bryan, G. H., and van den Heever, S. C.: Storm and Cloud Dynamics, Academic Press, second edition edn., 2010.

Curtius, J., Weigel, R., Vössing, H.-J., Wernli, H., Werner, A., Volk, C.-M., Konopka, P., Krebsbach, M., Schiller, C., Roiger, A., Schlager, H., Dreiling, V., and Borrmann, S.: Observations of meteoric material and implications for aerosol nucleation in the winter Arctic lower stratosphere derived from in situ particle measurements, Atmospheric Chemistry and Physics, 5, 3053–3069, https://doi.org/10.5194/acp-5-3053-2005, https://www.atmos-chem-phys.net/5/3053/2005/, 2005.

Deuflhard, P.: Newton Methods for Nonlinear Problems, vol. 35 of *Springer Series in Computational Mathematics*, Springer-Verlag, Berlin Heidelberg, https://doi.org/10.1007/978-3-642-23899-4, 2011.

Dixon, J. C.: The Shock Absorber Handbook, John Wiley & Sons Ltd, Chichester, second edition edn., 2007.

Emanuel, K. A.: Atmospheric Convection, Oxford University Press, https://books.google.de/books?id=VdaBBHEGAcMC, 1994.

Fay, J. A.: Molecular Thermodynamics, Engineering Sciences, Addison-Wesley, Reading, Massachusetts, 1965.

Feistel, R.: A Gibbs function for seawater thermodynamics for -6 to $80\,^{\circ}\mathrm{C}$ and salinity up to $120\,\mathrm{g\,kg^{-1}}$, Deep Sea Research Part I: Oceanographic Research Papers, 55, 1639 – 1671, https://doi.org/10.1016/j.dsr.2008.07.004, http://www.sciencedirect.com/science/article/pii/S0967063708001489, 2008.

Gettelman, A., Hoor, P., Pan, L. L., Randel, W. J., Hegglin, M. I., and Birner, T.: The Extratropical Upper Troposphere and Lower Stratosphere, Reviews of Geophysics, 49, https://doi.org/10.1029/2011RG000355, 2011.

Hallam, A.: Alfred Wegener and the Hypothesis of Continental Drift, Scientific American, 232, 88–97, http://www.jstor.org/stable/24949733, 1975.

https://doi.org/10.5194/acp-2020-361
Preprint. Discussion started: 4 May 2020

Atmospheric Chemistry and Physics Discussions

Hauf, T. and Höller, H.: Entropy and Potential Temperature, Journal of the Atmospheric Sciences, 44, 2887–2901, https://doi.org/10.1175/1520-0469(1987)044<2887:EAPT>2.0.CO;2, 1987.

Holton, J. R.: An Introduction to Dynamic Meteorology, vol. 88 of *International Geophysics Series*, Elsevier Academic Press, fourth edition edn., 2004.

Houghton, J.: The Physics of Atmospheres, Cambridge University Press, https://books.google.de/books?id=K9wGHim2DXwC, 2002.

Huang, K.: Statistical Mechanics, John Wiley & Sons, New York, second edn., 1987.

Jakob, M.: Die spezifische Wärme der Luft im Bereich von 0 bis 200 at und von -80 bis 250°, Mitteilungen aus der Physikalisch-Technischen Reichsanstalt, Zeitschr. f. techn. Physik, pp. 460–468, 1923.

Kondepudi, D. and Prigogine, I.: Modern Thermodynamics, John Wiley & Son, Chichester, 1998.

Köppen, W. P.: Über Luftmischung und potentielle Temperatur, in Anlehnung an die neueste Abhandlung von Herrn v. Helmholtz, http://snowcrystals.com, 1888.

Kunz, O. and Wagner, W.: The GERG-2008 Wide-Range Equation of State for Natural Gases and Other Mixtures: An Expansion of GERG-2004, J. Chem. Eng. Data, 57, 3032 – 3091, 2012.

Kutzbach, G.: The Thermal Theory of Cyclones: A History of Meteorological Thought in the Nineteenth Century, Meteorological Monographs, American Meteorological Society, https://books.google.de/books?id=bqXCDAAAQBAJ, 2016.

Lemmon, E. W., Jacobsen, R. T., Penoncello, S. G., and Friend, D. G.: Thermodynamic Properties of Air and Mixtures of Nitrogen, Argon, and Oxygen From 60 to 2000 K at Pressures to 2000 MPa, Journal of Physical and Chemical Reference Data, 29, 331–385, https://doi.org/10.1063/1.1285884, https://doi.org/10.1063/1.1285884, 2000.

Lemmon, E. W., Bell, I. H., Huber, M. L., and McLinden, M. O.: NIST Standard Reference Database 23: Reference Fluid Thermodynamic and Transport Properties-REFPROP, Version 10.0, National Institute of Standards and Technology, https://doi.org/https://dx.doi.org/10.18434/T4JS3C, https://www.nist.gov/srd/refprop, 2018.

Li, C. and Chen, X.: Simulating Nonhydrostatic Atmospheres on Planets (SNAP): Formulation, Validation, and Application to the Jovian Atmosphere, The Astrophysical Journal Supplement Series, 240, 37, https://doi.org/10.3847/1538-4365/aafdaa, 2019.

Lindzen, R. S.: Turbulence and stress owing to gravity wave and tidal breakdown, J. Geophys. Res., 86, 9707–9714, 1981.

Marquet, P.: Definition of a moist entropy potential temperature: application to FIRE-I data flights, Quarterly Journal of the Royal Meteorological Society, 137, 768–791, https://doi.org/10.1002/qj.787, 2011.

McDougall, T. J., Jackett, D. R., Wright, D. G., and Feistel, R.: Accurate and Computationally Efficient Algorithms for Potential Temperature and Density of Seawater, Journal of Atmospheric and Oceanic Technology, 20, 730–741, https://doi.org/10.1175/1520-0426(2003)20<730:AACEAF>2.0.CO;2, https://doi.org/10.1175/1520-0426(2003)20<730:AACEAF>2.0.CO;2, 2003.

Müller-Wodarg, I., Griffith, C. A., Lellouch, E., and Cravens, T. E.: Titan: Interior, Surface, Atmosphere, and Space Environment, vol. 14 of *Cambridge Planetary Science*, Cambridge University Press, 2014.

Newell, D. B., Cabiati, F., Fischer, J., Fujii, K., Karshenboim, S. G., Margolis, H. S., de Mirandés, E., Mohr, P. J., Nez, F., Pachucki, K., Quinn, T. J., Taylor, B. N., Wang, M., Wood, B. M., and Zhang, Z.: The CODATA 2017 values of h, e, k, and N_A for the revision of the SI, Metrologia, 55, L13–L16, https://doi.org/10.1088/1681-7575/aa950a, https://doi.org/10.1088/1681-7575/aa950a, 2018.

Ooyama, K. V.: A Thermodynamic Foundation for Modeling the Moist Atmosphere, Journal of the Atmospheric Sciences, 47, 2580–2593, https://doi.org/10.1175/1520-0469(1990)047<2580:ATFFMT>2.0.CO;2, https://doi.org/10.1175/1520-0469(1990)047<2580:ATFFMT>2.0.CO;2, 1990.

https://doi.org/10.5194/acp-2020-361
Preprint. Discussion started: 4 May 2020

Ooyama, K. V.: A Dynamic and Thermodynamic Foundation for Modeling the Moist Atmosphere with Parameterized Microphysics, Journal of the Atmospheric Sciences, 58, 2073–2102, https://doi.org/10.1175/1520-0469(2001)058<2073:ADATFF>2.0.CO;2, https://doi.org/10.1175/1520-0469(2001)058<2073:ADATFF>2.0.CO;2, 2001.

Palmer, T. N., Shutts, G. J., and Swinbank, R.: Alleviation of a systematic westerly bias in general circulation and numerical weather-prediction models through an orographic gravity wave drag parametrization, Q. J. R. Meteorol. Soc., 112, 1001–1039, 1986.

Plougonven, R. and Zhang, F.: Internal gravity waves from atmospheric jets and fronts, Rev. Geophys., 52, 33–76, https://doi.org/10.1002/2012RG000419, 2014.

Pruppacher, H. R. and Klett, J. D.: Microphysics of Clouds and Precipitation, vol. 18 of *Atmospheric and Oceanographic Sciences Library*, Kluwer Academic Publishers, Dordrecht, 2010.

Reinke-Kunze, C.: Alfred Wegener: Polarforscher und Entdecker der Kontinentaldrift, Lebensgeschichten aus der Wissenschaft, Birkhäuser Basel, https://books.google.de/books?id=u7edBgAAQBAJ, 2013.

Richardson, M. I., Toigo, A. D., and Newman, C. E.: PlanetWRF: A general purpose, local to global numerical model for planetary atmospheric and climate dynamics, Journal of Geophysical Research: Planets, 112, https://doi.org/10.1029/2006JE002825, https://agupubs.onlinelibrary.wiley.com/doi/abs/10.1029/2006JE002825, 2007.

Roebuck, J. R.: The Joule-Thomson Effect in Air, Proceedings of the American Academy of Arts and Sciences, 60, 537–596, http://www.jstor.org/stable/25130079, 1925.

Roebuck, J. R.: The Joule-Thomson Effect in Air. Second Paper, Proceedings of the American Academy of Arts and Sciences, 64, 287–334, http://www.jstor.org/stable/20026275, 1930.

Roedel, W. and Wagner, T.: Physik unserer Umwelt: Die Atmosphäre, Springer Berlin Heidelberg, https://doi.org/10.1007/978-3-642-15729-5, 2011.

Scheel, K. and Heuse, W.: Die spezifische Wärme der Luft bei Zimmertemperatur und bei tiefen Temperaturen, Annalen der Physik, 342, 79–95, https://doi.org/10.1002/andp.19113420106, https://onlinelibrary.wiley.com/doi/abs/10.1002/andp.19113420106, 1912.

Schmidt, R. and Wagner, W.: A new form of the equation of state for pure substances and its application to oxygen, Fluid Phase Equilibria, 19, 175 – 200, https://doi.org/https://doi.org/10.1016/0378-3812(85)87016-3, http://www.sciencedirect.com/science/article/pii/0378381285870163, 1985.

Schumann, U.: Atmospheric Physics; Background – Methods – Trends, Research Topics in Aerospace, Springer-Verlag, Berlin Heidelberg, https://doi.org/10.1007/978-3-642-30183-4, 2012.

Seinfeld, J. H. and Pandis, S. N.: Atmospheric Chemistry and Physics: From Air Pollution to Climate Change, A Wiley-Interscience publication, Wiley, https://books.google.de/books?id=tZEpAQAAMAAJ, 2006.

Span, R., Lemmon, E. W., Jacobsen, R. T., Wagner, W., and Yokozeki, A.: A Reference Equation of State for the Thermodynamic Properties of Nitrogen for Temperatures from 63.151 to 1000 K and Pressures to 2200 MPa, Journal of Physical and Chemical Reference Data, 29, 1361–1433, https://doi.org/10.1063/1.1349047, https://doi.org/10.1063/1.1349047, 2000.

Spichtinger, P.: Shallow cirrus convection - a source for ice supersaturation, Tellus A, 66, http://www.tellusa.net/index.php/tellusa/article/view/19937, 2014.

Swann, W. F. G. and Callendar, H. L.: VI. On the specific heats of air and carbon dioxide at atmospheric pressure by the continuous electric method at 20 °C and 100 °C, Philosophical Transactions of the Royal Society of London. Series A, Containing Papers of a Mathematical or Physical Character, 210, 199–238, https://doi.org/10.1098/rsta.1911.0006, https://royalsocietypublishing.org/doi/abs/10.1098/rsta.1911.0006, 1911.

https://doi.org/10.5194/acp-2020-361
Preprint. Discussion started: 4 May 2020

Swinbank, R. and Ortland, D. A.: Compilation of wind data for the (UARS) Reference Atmosphere Project, J. Geophys. Res., 108, D19, 4615, https://doi.org/10.1029/2002JD003135, 2003.

Tegeler, C., Span, R., and Wagner, W.: A New Equation of State for Argon Covering the Fluid Region for Temperatures from the Melting Line to 700 K at Pressures up to 1000 MPa, J. Phys. Chem. Ref. Data, 28, 779 – 850, 1999.

Tiesinga, E., Mohr, P. J., Newell, D. B., and Taylor, B. N.: The 2018 CODATA Recommended Values of the Fundamental Physical Constants, Web Version 8.1, Database developed by J. Baker, M. Douma, and S. Kotochigova. Available at http://physics.nist.gov/constants, 2020.

Tripoli, G. J. and Cotton, W. R.: The Use of lce-Liquid Water Potential Temperature as a Thermodynamic Variable In Deep Atmospheric Models, Monthly Weather Review, 109, 1094–1102, https://doi.org/10.1175/1520-0493(1981)109<1094:TUOLLW>2.0.CO;2, https://doi.org/10.1175/1520-0493(1981)109<1094:TUOLLW>2.0.CO;2, 1981.

Tsilingiris, P. T.: Thermophysical and transport properties of humid air at temperature range between 0 and 100 °C, Energy Conversion and Management, 49, 1098 – 1110, https://doi.org/https://doi.org/10.1016/j.enconman.2007.09.015, http://www.sciencedirect.com/science/article/pii/S0196890407003329, 2008.

United States Committee on Extension to the Standard Atmosphere: U.S. standard atmosphere, 1976, National Oceanic and Atmospheric Administration, U.S. Government Printing Office, Washington D. C., https://ntrs.nasa.gov/archive/nasa/casi.ntrs.nasa.gov/19770009539.pdf, 1976.

Vallis, G. K.: Atmospheric and Oceanic Fluid Dynamics, Cambridge University Press, Cambridge, U.K., 2006.

Vasserman, A. A., Kazavchinskii, Y. Z., and Rabinovich, V. A.: Thermophysical Properties of Air and Air Components, Academy of Sciences of the USSR, Israel Program for Scientific Translation Ltd., Jerusalem 1971, 1966.

von Bezold, W.: Zur Thermodynamik der Atmosphaere, pp. 1189 – 1206, Verlag der königlichen Akademie der Wissnschaften, Berlin, 1888.

von Helmholtz, H.: Über atmosphaerische Bewegungen, pp. 647 – 663, Verlag der königlichen Akademie der Wissnschaften, Berlin, 1888.

Wagner, W. and de Reuck, K. M.: Oxygen, International Thermodynamic Tables of the Fluid State, vol. 9 of *IUPAC Thermodynamic Tables Project*, Blackwell Science, Oxford, UK, 1987.

Wallace, J. M. and Hobbs, P. V.: Atmospheric Science, vol. 92 of *International Geophysics Series*, Academic Press, second edition edn., 2006.

Wegener, A.: Thermodynamik der Atmosphäre, J. A. Barth, Leipzig, 1911.

Wegener, A. and Wegener, K.: Vorlesung über Physik der Atmosphäre, J. A. Barth, Leipzig, 1935.

Weigel, R., Spichtinger, P., Mahnke, C., Klingebiel, M., Afchine, A., Petzold, A., Krämer, M., Costa, A., Molleker, S., Reutter, P., Szakáll, M., Port, M., Grulich, L., Jurkat, T., Minikin, A., and Borrmann, S.: Thermodynamic correction of particle concentrations measured by underwing probes on fast-flying aircraft, Atmospheric Measurement Techniques, 9, 5135–5162, https://doi.org/10.5194/amt-9-5135-2016, http://www.atmos-meas-tech.net/9/5135/2016/, 2016.

Wendisch, M. and Brenguier, J.-L.: Airborne Measurements for Environmental Research: Methods and Instruments, Wiley-VCH, Weinheim, https://doi.org/10.1002/9783527653218, 2013.

Witkowski, A. W.: I. Thermodynamic properties of air, The London, Edinburgh, and Dublin Philosophical Magazine and Journal of Science, 42, 1–37, https://doi.org/10.1080/14786449608620887, https://doi.org/10.1080/14786449608620887, 1896.

WMO: International Meteorological Tables, WMO-No.188.TP97, Secretariat of the World Meteorological Organization, Geneva, Switzerland, https://library.wmo.int/pmb_ged/wmo_188e.pdf, 1966.

Zdunkowski, W. and Bott, A.: Dynamics of the Atmosphere: A Course in Theoretical Meteorology, Cambridge University Press, https://books.google.de/books?id=ujOfdJxv_IQC, 2003.